

TABLE I—ASSOCIATION BETWEEN *SOCS-1* METHYLATION STATUS AND CLINICOPATHOLOGIC FEATURES AND CIMP STATUS IN GASTRIC CARCINOMAS

	<i>SOCS-1</i> methylation <sup>1</sup>		<i>p</i> -value <sup>2</sup>
	Positive	Negative	
Sex			
Male	24	28	0.572
Female	9	14	
Age			
≤65	9	15	0.437
>66	24	27	
T grade			
1, 2	11	22	0.099
3, 4	22	20	
N stage			
N0	5	18	0.009
N1, 2, 3	28	24	
Stage			
Stage I, II	10	23	0.034
Stage III, IV	23	19	
Histology			
Intestinal	17	22	0.941
Diffuse	16	20	
Histology			
Intestinal and diffuse-adherent	24	27	0.437
Diffuse-scattered	9	15	

<sup>1</sup>Methylation status of the *SOCS-1* gene was examined by MSP3' analysis.—<sup>2</sup>Fisher's exact test.

demethylating agents might control tumor formation and progression of GC.

In conclusion, our results suggest that *SOCS-1* is subject to epigenetic silencing by DNA methylation in a considerable proportion of GCs and that epigenetic inactivation of *SOCS-1* by hypermethylation may be involved in development, progression and metastasis of GC. Although additional studies are needed to understand the biologic significance of *SOCS-1* inactivation in gastric tumorigenesis, our findings suggest that *SOCS-1* methylation could be a useful molecular marker for detection and evaluation of progression and metastatic potential of GC. Frequent

TABLE II—ASSOCIATION BETWEEN *SOCS-1* MRNA EXPRESSION AND METHYLATION STATUS AND CLINICOPATHOLOGIC FEATURES IN GASTRIC CARCINOMAS

	<i>SOCS-1</i> reduced expression		<i>p</i> value <sup>1</sup>
	Positive	Negative	
Sex			
Male	19	15	0.225
Female	6	10	
Age			
≤65	8	11	0.382
>66	17	14	
T grade			
1, 2	7	12	0.145
3, 4	18	13	
N grade			
N0	3	11	0.013
N1, N2, N3	22	14	
Stage			
Stage I, II	4	15	0.002
Stage III, IV	21	10	
Histology			
Intestinal	13	13	1.000
Diffuse	12	12	
Histology			
Intestinal and diffuse-adherent	15	18	0.370
Diffuse-scattered	10	7	
<i>SOCS-1</i> methylation			
Positive	17	6	0.002
Negative	8	19	

<sup>1</sup>Fisher's exact test.

constitutive activation of the JAK/STAT pathway by hypermethylation of the *SOCS-1* gene may be a molecular target for treatment of GC.

#### ACKNOWLEDGEMENTS

We thank Mr. M. Takatani for his excellent technical assistance and advice. This work was carried out with the kind cooperation of the Research Center for Molecular Medicine, Faculty of Medicine, Hiroshima University.

#### REFERENCES

- Yasui W, Yokozaki H, Fujimoto J, Naka K, Kuniyasu H, Tahara E. Genetic and epigenetic alterations in multistep carcinogenesis of the stomach. *J Gastroenterol* 2000;35:111–5.
- Jones PA, Baylin SB. The fundamental role of epigenetic events in cancer. *Nat Rev Genet* 2002;3:415–28.
- Baylin SB, Herman JG, Graff JR, Vertino PM, Issa JP. Alterations in DNA methylation: a fundamental aspect of neoplasia. *Adv Cancer Res* 1998;72:141–96.
- Fleisher AS, Esteller M, Wang S, Tamura G, Suzuki H, Yin J, Zou TT, Abraham JM, Kong D, Smolinski KN, Shi YQ, Rhyu MG, et al. Hypermethylation of the hMLH1 gene promoter in human gastric cancers with microsatellite instability. *Cancer Res* 1999;59:1090–5.
- Leung SY, Yuen ST, Chung LP, Chu KM, Chan AS, Ho JC. hMLH1 promoter methylation and lack of hMLH1 expression in sporadic gastric carcinomas with high-frequency microsatellite instability. *Cancer Res* 1999;59:159–64.
- Shim YH, Kang GH, Ro JY. Correlation of p16 hypermethylation with p16 protein loss in sporadic gastric carcinomas. *Lab Invest* 2000;80:689–95.
- Tamura G, Yin J, Wang S, Fleisher AS, Zou T, Abraham JM, Kong D, Smolinski KN, Wilson KT, James SP, Silverberg SG, Nishizuka S, et al. E-Cadherin gene promoter hypermethylation in primary human gastric carcinomas. *J Natl Cancer Inst* 2000;92:569–73.
- Song SH, Jong HS, Choi HH, Inoue H, Tanabe T, Kim NK, Bang YJ. Transcriptional silencing of Cyclooxygenase-2 by hyper-methylation of the 5' CpG island in human gastric carcinoma cells. *Cancer Res* 2001;61:4628–35.
- Byun DS, Lee MG, Chae KS, Ryu BG, Chi SG. Frequent epigenetic inactivation of RASSF1A by aberrant promoter hypermethylation in human gastric adenocarcinoma. *Cancer Res* 2001;61:7034–8.
- Kang YH, Lee HS, Kim WH. Promoter methylation and silencing of PTEN in gastric carcinoma. *Lab Invest* 2002;82:285–91.
- Sato K, Tamura G, Tsuchiya T, Endoh Y, Usuba O, Kimura W, Motoyama T. Frequent loss of expression without sequence mutations of the DCC gene in primary gastric cancer. *Br J Cancer* 2001;85:199–203.
- Kaneda A, Kaminishi M, Nakanishi Y, Sugimura T, Ushijima T. Reduced expression of the insulin-induced protein 1 and p41 Arp2/3 complex genes in human gastric cancers. *Int J Cancer* 2002;100:57–62.
- Kaneda A, Kaminishi M, Yanagihara K, Sugimura T, Ushijima T. Identification of silencing of nine genes in human gastric cancers. *Cancer Res* 2002;62:6645–50.
- Oue N, Shigeishi H, Kuniyasu H, Yokozaki H, Kuraoka K, Ito R, Yasui W. Promoter hypermethylation of MGMT is associated with protein loss in gastric carcinoma. *Int J Cancer* 2001;93:805–9.
- Oue N, Motoshita J, Yokozaki H, Hayashi K, Tahara E, Taniyama K, Matsusaki K, Yasui W. Distinct promoter hypermethylation of p16INK4a, CDH1, and RAR-beta in intestinal, diffuse-adherent, and diffuse-scattered type gastric carcinomas. *J Pathol* 2002;198:55–9.
- Oue N, Matsumura S, Nakayama H, Kitadai Y, Taniyama K, Matsusaki K, Yasui W. Reduced expression of the TSP1 gene and its association with promoter hypermethylation in gastric carcinoma. *Oncology* 2003;64:423–9.
- Hamai Y, Oue N, Mitani Y, Nakayama H, Ito R, Matsusaki K, Yoshida K, Toge T, Yasui W. DNA hypermethylation and histone hypoacetylation of the HMTF gene are associated with reduced expression in gastric carcinoma. *Cancer Sci* 2003;94:692–8.
- Oshimo Y, Oue N, Mitani Y, Nakayama H, Kitadai Y, Yoshida K, Ito Y, Chayama K, Yasui W. Frequent loss of RUNX3 expression by promoter hypermethylation in gastric carcinoma. *Pathobiology* 2004;71:137–43.
- Oshimo Y, Oue N, Mitani Y, Nakayama H, Kitadai Y, Yoshida K, Chayama K, Yasui W. Frequent epigenetic inactivation of RIZ1 by

- promoter hypermethylation in human gastric carcinoma. *Int J Cancer* 2004;110:212–8.
20. Kang GH, Lee S, Kim JS, Jung HY. Profile of aberrant CpG island methylation along the multistep pathway of gastric carcinogenesis. *Lab Invest* 2003;83:635–41.
  21. Chan AO, Lam SK, Wong BC, Wong WM, Yuen MF, Yeung YH, Hui WM, Rashid A, Kwong YL. Promoter methylation of E-cadherin gene in gastric mucosa associated with *Helicobacter pylori* infection and in gastric cancer. *Gut* 2003;52:502–6.
  22. Tanaka M, Kitajima Y, Edakuni G, Sato S, Miyazaki K. Abnormal expression of E-cadherin and beta-catenin may be a molecular marker of submucosal invasion and lymph node metastasis in early gastric cancer. *Br J Surg* 2002;89:236–44.
  23. Yamashita K, Mimori K, Inoue H, Mori M, Sidransky D. A tumor-suppressive role for trypsin in human cancer progression. *Cancer Res* 2003;63:6575–8.
  24. Darnell JE Jr, Kerr IM, Stark GR. Jak-STAT pathways and transcriptional activation in response to IFNs and other extracellular signaling proteins. *Science* 1994;264:1415–21.
  25. Bromberg JF, Wrzeszczynska MH, Devgan G, Zhao Y, Pestell RG, Albanese C, Darnell JE Jr. Stat3 as an oncogene. *Cell* 1999;98:295–303.
  26. Lacronique V, Boureux A, Valle VD, Poirel H, Quang CT, Mauchauffe M, Berthou C, Lessard M, Berger R, Ghysdael J, Bernard OA. A TEL-JAK2 fusion protein with constitutive kinase activity in human leukemia. *Science* 1997;278:1309–12.
  27. Wen Z, Zhong Z, Darnell JE Jr. Maximal activation of transcription by Stat1 and Stat3 requires both tyrosine and serine phosphorylation. *Cell* 1995;82:241–50.
  28. Kile BT, Schulman BA, Alexander WS, Nicola NA, Martin HM, Hilton DJ. The SOCS box: a tale of destruction and degradation. *Trends Biochem Sci* 2002;27:235–41.
  29. Greenhalgh CJ, Miller ME, Hilton DJ, Lund PK. Suppressors of cytokine signaling: Relevance to gastrointestinal function and disease. *Gastroenterology* 2002;123:2064–81.
  30. Starr R, Hilton DJ. SOCS: suppressors of cytokine signalling. *Int J Biochem Cell Biol* 1998;30:1081–5.
  31. Starr R, Willson TA, Viney EM, Murray LJ, Rayner JR, Jenkins BJ, Gonda TJ, Alexander WS, Metcalf D, Nicola NA, Hilton DJ. A family of cytokine-inducible inhibitors of signalling. *Nature* 1997;387:917–21.
  32. Endo TA, Masuhara M, Yokouchi M, Suzuki R, Sakamoto H, Mitsui K, Matsumoto A, Tanimura S, Ohtsubo M, Misawa H, Miyazaki T, Leonor N, et al. A new protein containing an SH2 domain that inhibits JAK kinases. *Nature* 1997;387:921–4.
  33. Naka T, Narazaki M, Hirata M, Matsumoto T, Minamoto S, Aono A, Nishimoto N, Kajita T, Taga T, Yoshizaki K, Akira S, Kishimoto T. Structure and function of a new STAT-induced STAT inhibitor. *Nature* 1997;387:924–9.
  34. Yoshikawa H, Matsubara K, Qian GS, Jackson P, Groopman JD, Manning JE, Harris CC, Herman JG. SOCS-1, a negative regulator of the JAK/STAT pathway, is silenced by methylation in human hepatocellular carcinoma and shows growth-suppression activity. *Nat Genet* 2001;28:29–35.
  35. Nagai H, Naka T, Terada Y, Komazaki T, Yabe A, Jin E, Kawanami O, Kishimoto T, Konishi N, Nakamura M, Kobayashi Y, Emi M. Hypermethylation associated with inactivation of the SOCS-1 gene, a JAK/STAT inhibitor, in human hepatoblastomas. *J Hum Genet* 2003;48:65–9.
  36. Galm O, Yoshikawa H, Esteller M, Osieka R, Herman JG. SOCS-1, a negative regulator of cytokine signaling, is frequently silenced by methylation in multiple myeloma. *Blood* 2003;101:2784–8.
  37. Chen CY, Tsay W, Tang JL, Shen HL, Lin SW, Huang SY, Yao M, Chen YC, Shen MC, Wang CH, Tien HF. SOCS1 methylation in patients with newly diagnosed acute myeloid leukemia. *Genes Chromosomes Cancer* 2003;37:300–5.
  38. Fukushima N, Sato N, Sahin F, Su GH, Hruban RH, Goggins M. Aberrant methylation of suppressor of cytokine signalling-1 (SOCS-1) gene in pancreatic ductal neoplasms. *Br J Cancer* 2003;89:338–43.
  39. Roitapel R, Ilangumaran S, Neale C, La Rose J, Ho JM, Nguyen MH, Barber D, Dubreuil P, de Sepulveda P. The tumor suppressor activity of SOCS-1. *Oncogene* 2002;21:4351–62.
  40. Lauren P. The two histological main types of gastric carcinoma. Diffuse and so-called intestinal type carcinoma: an attempt at histological classification. *Acta Pathol Microbiol Scand* 1965;64:31–49.
  41. Shimoyama Y, Hirohashi S. Expression of E- and P-cadherin in gastric carcinomas. *Cancer Res* 1991;51:2185–92.
  42. Sobin LH, Wittekind CH, eds. TNM classification of malignant tumors, 6th ed. New York: Wiley-Liss, 2002. 65–8.
  43. Herman JG, Graff JR, Myohanen S, Nelkin BD, Baylin SB. Methylation-specific PCR: a novel PCR assay for methylation status of CpG islands. *Proc Natl Acad Sci USA* 1996;93:9821–6.
  44. Kang GH, Shim YH, Jung HY, Kim WH, Ro JY, Rhyu MG. CpG island methylation in premalignant stages of gastric carcinoma. *Cancer Res* 2001;61:2847–51.
  45. To KF, Leung WK, Lee TL, Yu J, Tong JH, Chan MW, Ng EK, Chung SC, Sung JJ. Promoter hypermethylation of tumor-related genes in gastric intestinal metaplasia of patients with and without gastric cancer. *Int J Cancer* 2002;102:623–8.
  46. Waki T, Tamura G, Tsuchiya T, Sato K, Nishizuka S, Motoyama T. Promoter methylation status of E-cadherin, hMLH1, and p16 genes in nonneoplastic gastric epithelia. *Am J Pathol* 2002;161:399–403.
  47. Ahuja N, Issa JP. Aging, methylation and cancer. *Histol Histopathol* 2000;15:835–42.
  48. Melzner I, Moller P. Silencing of the SOCS-1 gene by CpG methylation? *Blood* 2003;102:1554–5.
  49. Ito R, Yasui W, Kuniyasu H, Yokozaki H, Tahara E. Expression of interleukin-6 and its effect on the cell growth of gastric carcinoma cell lines. *Jpn J Cancer Res* 1997;88:953–8.
  50. Wu CW, Wang SR, Chao MF, Wu TC, Lui WY, P'eng FK, Chi CW. Serum interleukin-6 levels reflect disease status of gastric cancer. *Am J Gastroenterol* 1996;91:1417–22.
  51. De Vita F, Romano C, Orditura M, Galizia G, Martinelli E, Lieto E, Catalano G. Interleukin-6 serum level correlates with survival in advanced gastrointestinal cancer patients but is not an independent prognostic indicator. *J Interferon Cytokine Res* 2001;21:45–52.
  52. Katakaki A, Sotirianakos S, Memos N, Karayiannis M, Messaris E, Leandros E, Manouras A, Androulakis G. P53 and C-FOS overexpression in patients with thyroid cancer: an immunohistochemical study. *Neoplasia* 2003;50:26–30.
  53. Cameron EE, Bachman KE, Myohanen S, Herman JG, Baylin SB. Synergy of demethylation and histone deacetylase inhibition in the re-expression of genes silenced in cancer. *Nat Genet* 1999;21:103–7.

## Expression of *POT1* is Associated with Tumor Stage and Telomere Length in Gastric Carcinoma

Tomohiro Kondo,<sup>1</sup> Naohide Oue,<sup>1</sup> Kazuhiro Yoshida,<sup>2</sup> Yoshitsugu Mitani,<sup>1</sup> Kazuhito Naka,<sup>3</sup> Hirofumi Nakayama,<sup>1</sup> and Wataru Yasui<sup>1</sup>

<sup>1</sup>Department of Molecular Pathology, Hiroshima University Graduate School of Biomedical Sciences, Hiroshima; <sup>2</sup>Department of Surgical Oncology, Research Institute for Radiation Biology and Medicine, Hiroshima University, Hiroshima; and <sup>3</sup>Department of Molecular Biology, Okayama University Graduate School of Medicine and Dentistry, Okayama, Japan

### ABSTRACT

Pot1, a telomere end-binding protein in fission yeast and human, is proposed not only to cap telomeres but also to recruit telomerase to the ends of chromosomes. No study has been performed regarding Pot1 expression status in human cancers. Thus, we examined *POT1* mRNA expression in 51 gastric cancer (GC) tissues and evaluated telomere length and 3' telomeric overhang signals in 20 of the 51 GC tissues. Quantitative reverse transcription-PCR analysis showed that *POT1* expression levels in the tumor relative to those in nonneoplastic mucosa (T/N ratio) were significantly higher in stage III/IV tumors than in stage I/II tumors ( $P = 0.005$ ). Down-regulation of *POT1* ( $T/N < 0.5$ ) was observed more frequently in stage I/II GC (52.4%, 11 of 21) than in stage III/IV GC (23.3%, 7 of 30;  $P = 0.033$ ), whereas up-regulation of *POT1* ( $T/N > 2.0$ ) was observed more frequently in stage III/IV GC (33.3%, 10 of 30) than in stage I/II GC (9.5%, 2 of 21;  $P = 0.048$ ). *POT1* expression levels showed decreased in accordance with telomere shortening ( $r = 0.713$ ,  $P = 0.002$ ). In-gel hybridization analysis showed that 3' telomeric overhang signals decreased in accordance with decreases in *POT1* expression levels ( $r = 0.696$ ,  $P = 0.002$ ) and telomere shortening ( $r = 0.570$ ,  $P = 0.013$ ). Reduced *POT1* expression was observed in GC cell lines with telomeres shortened by treatment with azidothymidine. In addition, inhibition of Pot1 by antisense oligonucleotides led to telomere shortening as well as inhibition of telomerase activity in GC cells. Moreover, inhibition of Pot1 decreased 3' overhang signals and increased the frequency of anaphase bridge ( $P = 0.0005$ ). These data suggest that Pot1 may play an important role in regulation of telomere length and that inhibition of Pot1 may induce telomere dysfunction. Moreover, changes in *POT1* expression levels may be associated with stomach carcinogenesis and GC progression.

### INTRODUCTION

Telomeres are distinctive structures consisting of a repetitive DNA sequence (TTAGGG) and associated proteins that cap the ends of linear chromosomes. Telomeres enable cells to distinguish chromosomal ends from double-strand breaks in the genome. Mammalian telomeric DNA is mostly composed of double-stranded 5'-TTAGGG-3' repeats and terminates with a single-stranded overhang of the G-rich strand (1-3). In human somatic cells, telomeres have 500-3000 TTAGGG repeats, but telomeres shorten gradually with age (4-6). In contrast, telomeres of germ line and cancer cells do not shorten, consistent with the behavior of immortal and unicellular organisms. The telomeres of immortal cells are maintained by telomerase, which is able to extend 3' telomeric overhangs, or by recombination (7-10). Telomerase activity confers cell immortality through stabilization of the chromosome, and it participates in the develop-

ment of the majority of human cancers. We have shown that telomerase activity occurs in early-stage gastric cancer (GC; Ref. 11) and that telomerase reverse transcriptase expression is required for telomerase activity in the initiation of carcinogenesis in the stomach (12).

A single-stranded telomeric DNA binding protein, protection of telomeres (Pot1), has been identified in fission yeast and human (13). In fission yeast, most cells lacking Pot1 die because of sequence loss and end-to-end chromosomal fusion, although a few survivors emerge that have circularized all three chromosomes, thereby bypassing the requirement for chromosomal end maintenance. Purified fission yeast and human Pot1 proteins bind specifically to the G-rich strand of their own telomeric DNA but not to the complementary C-rich strand or double-stranded telomeric DNA, consistent with a role in binding to the 3' telomeric overhang at the ends of telomeres *in vivo*. In *Saccharomyces cerevisiae*, the single-stranded telomeric DNA binding protein Cdc13 not only caps telomeres but also recruits telomerase to the ends of chromosomes (14, 15). Therefore, Pot1 is thought to be involved in this dual task (13, 16-18). A recent study indicated that each Pot1 binds to one telomeric repeat and coats the entire single-stranded overhang of the telomere in *Schizosaccharomyces pombe* (18). However, no study has investigated Pot1 expression status and its association with telomere length in human cancers including GC.

We investigated expression of the *POT1* gene and its relation to telomere length and 3' telomeric overhang in GC tissues. Moreover, we studied the relation between *POT1* gene expression levels and telomere length in GC cell lines using azidothymidine (AZT) and *POT1* antisense oligonucleotides because AZT causes telomere shortening by inhibiting telomerase activity (19-22). In addition, we investigated alteration of 3' telomeric overhang signals and the frequency of anaphase bridges in GC cells treated with *POT1* antisense oligonucleotides.

### MATERIALS AND METHODS

**Samples.** Fifty-one pairs of GC tissues and corresponding nonneoplastic mucosae were studied. Specimens were removed surgically, frozen immediately in liquid nitrogen, and stored at  $-80^{\circ}\text{C}$  until use. We confirmed microscopically that the carcinoma specimens consisted mainly of carcinoma tissue and that the nonneoplastic mucosae showed no invasion by carcinoma cells or significant inflammatory involvement. Histological classification and tumor staging were done according to the Lauren classification system (23) and tumor-node-metastasis (24) classification systems. From among a total 51 GC cases, we randomly selected 20 cases in which high molecular weight DNA was available to evaluate telomere lengths and 3' telomeric overhang signals.

**GC Cell Lines.** Two cell lines derived from human GC were used: MKN-28 and MKN-74 derived from well-differentiated adenocarcinomas and kindly provided by Dr. Toshimitsu Suzuki. Both cell lines were maintained in RPMI 1640 (Nissui Pharmaceutical Co., Ltd., Tokyo, Japan) containing 10% fetal bovine serum (Whittaker, Walkersville, MA) in a humidified atmosphere of 5%  $\text{CO}_2$  and 95% air at  $37^{\circ}\text{C}$ .

**Quantitative Reverse Transcription (RT)-PCR.** Total RNA was extracted with the RNeasy Mini Kit (Qiagen, Valencia, CA). Total RNA (1  $\mu\text{g}$ ) was converted to cDNA with the First Strand cDNA Synthesis kit (Amersham Pharmacia Biotech, Uppsala, Sweden). PCRs were performed with the SYBR

Received 4/30/03; revised 10/21/03; accepted 11/6/03.

Grant support: Grants-in-Aid for Cancer Research from the Ministry of Education, Culture, Science, Sports, and Technology of Japan and from the Ministry of Health, Labor, and Welfare of Japan.

The costs of publication of this article were defrayed in part by the payment of page charges. This article must therefore be hereby marked *advertisement* in accordance with 18 U.S.C. Section 1734 solely to indicate this fact.

Requests for reprints: Dr. Wataru Yasui, Department of Molecular Pathology, Hiroshima University Graduate School of Biomedical Sciences, 1-2-3 Kasumi, Minami-ku, Hiroshima 734-8551, Japan. Fax: 81-82-257-5149; E-mail: wyasui@hiroshima-u.ac.jp.

Green PCR Core Reagent kit (Applied Biosystems, Foster City, CA). Real-time detection of the emission intensity of SYBR Green bound to double-stranded DNAs was by the ABI PRISM 7700 Sequence Detection System (Applied Biosystems). *POT1* cDNA and internal control cDNA ( $\beta$ -actin gene, *ACTB*) were PCR amplified separately. Relative gene expression was determined by the threshold cycles for the *POT1* gene and *ACTB* gene. Reference samples (GC cell line, HSC-39) were included on each assay plate to verify plate-to-plate consistency. Plates were normalized to each other by these reference samples. PCR amplification was performed according to the manufacturer's instructions in 96-well optical trays with caps with a 25- $\mu$ l final reaction mixture. Quantitative RT-PCRs were performed in triplicate for each sample primer set, and the mean of the three experiments was used as the relative quantification value. *POT1* primer sequences were 5'-TCAGTCTGT-TAAACTTCATTGCC-3' and 5'-TGCACCATCCTGAAAAATTATATCC-3'. *ACTB* primer sequences were 5'-TCACCGAGCGCGCT-3' and 5'-TAATGTCACGCACGATTTCCC-3'.

**Telomere Restriction Fragment Length Analysis.** High molecular weight genomic DNA was extracted with a DNA Extraction kit (Stratagene Cloning System, La Jolla, CA). Tissue DNA was digested with *HinfI*, electrophoresed on 0.6% agarose gels, and blotted onto nitrocellulose filters. The filters were hybridized with a telomeric DNA probe and then autoradiographed. We estimated the telomere length as the peak signal using Kodak Digital Science 1D software (Eastman Kodak Company, New Haven, CT).

**3' Telomeric Overhang Assay (In-Gel Hybridization).** In-gel hybridization to measure 3' telomeric overhangs was carried out as described in Wellinger *et al.* (25). DNA samples were digested with *HinfI* and electrophoresed on 0.6% agarose gels. The gels were dried with a gel dryer for 24–28 min at room temperature. The very thin gels were then hybridized for 16 h at 37°C to end-labeled oligonucleotides in hybridization buffer. [TTAGGG]<sub>4</sub> and [CCCTAA]<sub>4</sub> oligonucleotide probes were end-labeled with  $\gamma$ -<sup>32</sup>P-ATP and T4 polynucleotide kinase. After removal of excess hybridization buffer, gels were washed twice with 0.25 $\times$  SSC for 1.5 h at room temperature, followed by 2-h washes at 30°C. After sequential native gel hybridization, dried gels were alkali-denatured in 0.15 M NaCl, 0.5 M NaOH for 25 min, neutralized in 0.15 M NaCl, 0.5 M Tris-HCl (pH 8.0) for 20 min, and reprobed. Image analysis and quantitation were performed with a Fuji Film BAS 2000 Bio-Imaging Analysis System and NIH Image.

**Telomeric Repeat Amplification Protocol Assay.** Telomeric repeat amplification protocol assay was done with a TRAPEZE Telomerase Detection kit (Intergen Company, Oxford, United Kingdom). Intensity of the telomeric repeat amplification protocol product bands and of the internal control bands was determined with the use of NIH Image.

**Telomere Shortening Assay.** We harvested MKN-28 and MKN-74 cells maintained at 37°C under 5% CO<sub>2</sub> in RPMI 1640 and 10% fetal bovine serum. Cells were pretreated for 5 and 10 days with medium exchange and addition of AZT (100  $\mu$ M) each day before being used for experiments.

**POT1 Antisense Oligonucleotides.** The 24-mer phosphorothioate oligonucleotide antisense sequence of the first 24 nucleotides of *POT1* was synthesized and purified by reverse-phase high-performance liquid chromatography (Especk Oligo Service, Tsukuba, Japan). The sequence was 5'-TTGTTGCTG-GAACCAAAGACATTG-3', and for control, complementary (sense) oligonucleotides were synthesized as 5'-CAATGTCCTTTGGTTCCAGCAACAA-3'. We harvested MKN-28 cells maintained at 37°C under 5% CO<sub>2</sub> in RPMI 1640 and 10% fetal bovine serum. Cells were pretreated with 2.5  $\mu$ M antisense or sense oligonucleotides in Lipofectamine (Invitrogen-Life Technologies, Inc., Carlsbad, CA) for 4 and 8 days by medium exchange and addition of antisense or sense oligonucleotides every 2 days before being used for experiments.

**Anaphase Bridges.** H&E-stained cultures or tissue sections were examined for anaphase bridges under a light microscope at  $\times$ 100 magnification. The anaphase bridge index (ABI) was determined by dividing the number of anaphases with bridges by the total number of anaphases. Anaphase bridging was defined as reported previously (26). Two investigators independently scored a minimum of 10 anaphases/sample.

**Statistical Analysis.** Statistical significance was assessed by Fisher's exact test, Mann-Whitney *U* test, Spearman's rank correlation test, or unpaired *t* test. Statview 5.0 Macintosh software was used. All tests were two-sided. A *P* of <0.05 was regarded as statistically significant.

**RESULTS**

**POT1 Expression Levels Increase with Tumor Stage.** Expression levels of *POT1* were measured by quantitative RT-PCR in the 51 cases of GC. We calculated the ratio of *POT1* mRNA expression levels in GC tissues relative to levels in nonneoplastic mucosae (T/N ratio). The T/N ratios were significantly higher in stage III/IV cancers than in stage I/II cancers (*P* = 0.005, Mann-Whitney *U* test; Fig. 1A). We considered a T/N > 2.0 to represent up-regulation and a T/N < 0.5 to represent down-regulation. Up-regulation of *POT1* was found in 12 (23.5%) of the 51 cases, and down-regulation was found in 18 (35.3%) of the 51 cases. Down-regulation of *POT1* was more frequent in stage I/II tumors (52.4%, 11 of 21) than in stage III/IV tumors (23.3%, 7 of 30; *P* = 0.033, Fisher's exact test; Table 1),

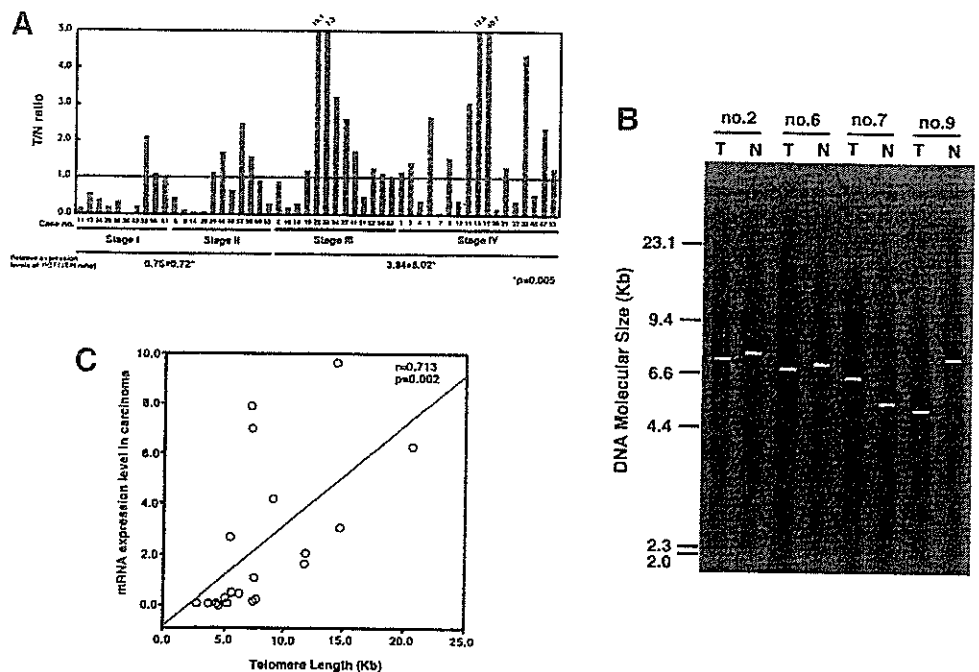


Fig. 1. *POT1* expression levels in gastric cancer (GC) and association with telomere length. **A**, distribution of *POT1* expression in the 51 cases of GC. T/N ratio stage I/II: 0.75  $\pm$  0.72; T/N ratio stage III/IV: 3.84  $\pm$  8.02, *P* = 0.005 by Mann-Whitney *U* test. **B**, representative telomere restriction fragment length analysis. Telomere lengths were determined in tumor tissues (T) and corresponding nonneoplastic mucosae (N). Horizontal white bars show the average length. **C**, *POT1* expression levels in tumor tissues correlate positively with telomere length (*r* = 0.713, *P* = 0.002 by Spearman's rank correlation test). T/N ratio = *POT1* mRNA expression levels in GC tissue relative to levels in corresponding nonneoplastic mucosa.

Table 1 Clinicopathological features of gastric cancers (n = 51) in relation to POT1 expression levels<sup>a</sup>

	Down-regulation (T/N <0.5)	No change (T/N = 0.5-2.0)	Up-regulation (T/N >2.0)	P
Histology <sup>b</sup>				
Intestinal	9 (36.0%)	9 (36.0%)	7 (28.0%)	n.s. <sup>c</sup>
Diffuse	9 (34.6%)	12 (46.2%)	5 (19.2%)	
T-grade <sup>d</sup>				
T <sub>1,2</sub>	12 (50.0%)	9 (37.5%)	3 (12.5%)	0.038 <sup>e</sup>
T <sub>3,4</sub>	6 (22.2%)	12 (44.5%)	9 (33.3%)	
N-grade <sup>d</sup>				
N <sub>0</sub>	6 (46.2%)	5 (38.4%)	2 (15.4%)	n.s.
N <sub>1,2,3</sub>	12 (31.6%)	16 (42.1%)	10 (26.3%)	
Stage <sup>d</sup>				
I, II	11 (52.4%)	8 (38.1%)	2 (9.50%)	0.033 <sup>c</sup> 0.048 <sup>f</sup>
III, IV	7 (23.3%)	13 (43.4%)	10 (33.3%)	

<sup>a</sup> T/N ratio = POT1 mRNA expression levels in GC tissue relative to levels in corresponding nonneoplastic mucosa.

<sup>b</sup> According to the Lauren criteria (23).

<sup>c</sup> n.s., not significant.

<sup>d</sup> According to the criteria of the tumor-node-metastasis stage classification system (24).

<sup>e</sup> By Fisher's exact test, for down-regulation versus no change and up-regulation.

<sup>f</sup> By Fisher's exact test, for down-regulation and no change versus up-regulation.

whereas up-regulation of POT1 was more frequent in stage III/IV tumors (33.3%, 10 of 30) than in stage I/II tumors (9.5%, 2 of 21;  $P = 0.048$ , Fisher's exact test; Table 1). In addition, down-regulation of POT1 was observed preferentially in low T grade (depth of invasion) cancers ( $P = 0.038$ , Fisher's exact test; Table 1). No association was found between POT1 expression level and N grade (degree of lymph node metastasis) or histological type (Table 1).

**Positive Correlation between POT1 Expression Levels and Telomere Length.** For association between POT1 expression levels and telomere length in GC tissues, telomere length was examined by Southern blotting analysis in 20 of the 51 cases (Fig. 1B). POT1 expression levels in GC tissue decreased in accordance with telomere shortening ( $r = 0.713$ ,  $P = 0.002$ , Spearman's rank correlation test; Fig. 1C).

**Positive Correlation between POT1 Expression Levels and 3' Telomeric Overhang Signals.** 3' overhang signals were examined by in-gel hybridization analysis in the same 20 GC tissues in which telomere lengths were measured (Fig. 2A). 3' overhang signals reduced in accordance with reduced POT1 expression levels ( $r = 0.696$ ,  $P = 0.002$ , Spearman's rank correlation test; Fig. 2B) and telomere shortening ( $r = 0.570$ ,  $P = 0.013$ , Spearman's rank correlation test; Fig. 2C).

**AZT Inhibition of POT1 Expression in GC Cells.** To confirm the positive correlation between POT1 expression levels and telomere length, we measured POT1 expression levels in GC cells in which telomeres were shortened by AZT. AZT inhibited telomerase activity and shortened telomeres (Fig. 3, A and B). Telomerase activity was inhibited with AZT by 68% after 5 days and 82% after 10 days in MKN-28 cells and by 23% after 5 days and 94% after 10 days in MKN-74 cells. AZT reduced telomere length from 3.9 to 3.7 Kb after 5 days and to 3.4 Kb after 10 days in MKN-28 cells and from 3.6 to 3.1 Kb after 5 days and to 2.7 Kb after 10 days in MKN-74 cells. Quantitative RT-PCR analysis showed POT1 expression to be down-regulated in AZT-treated cells (Fig. 3C). Expression of POT1 in AZT-treated MKN-28 cells was 29% of that in nontreated cells after

Fig. 2. 3' Telomeric overhang signals were associated with POT1 expression levels and telomere lengths. A, representative in-gel hybridization assay. The top left panel shows native gel probed with [CCCTAA]<sub>4</sub>, and the top right panel shows denatured gel probed with [CCCTAA]<sub>4</sub>. The bottom left panel shows native gel probed with [TTAGGG]<sub>4</sub>, and the bottom right panel shows denatured gel probed with [TTAGGG]<sub>4</sub>. Signals were expressed relative to the signal in MKN-74 gastric cancer cells. B, POT1 expression levels in tumor tissues correlate positively with 3' telomeric overhang signals in gastric cancer tissues ( $r = 0.696$ ,  $P = 0.002$  by Spearman's rank correlation test). C, telomere lengths correlate positively with 3' telomeric overhang signals in gastric cancer tissues ( $r = 0.570$ ,  $P = 0.013$  by Spearman's rank correlation test).

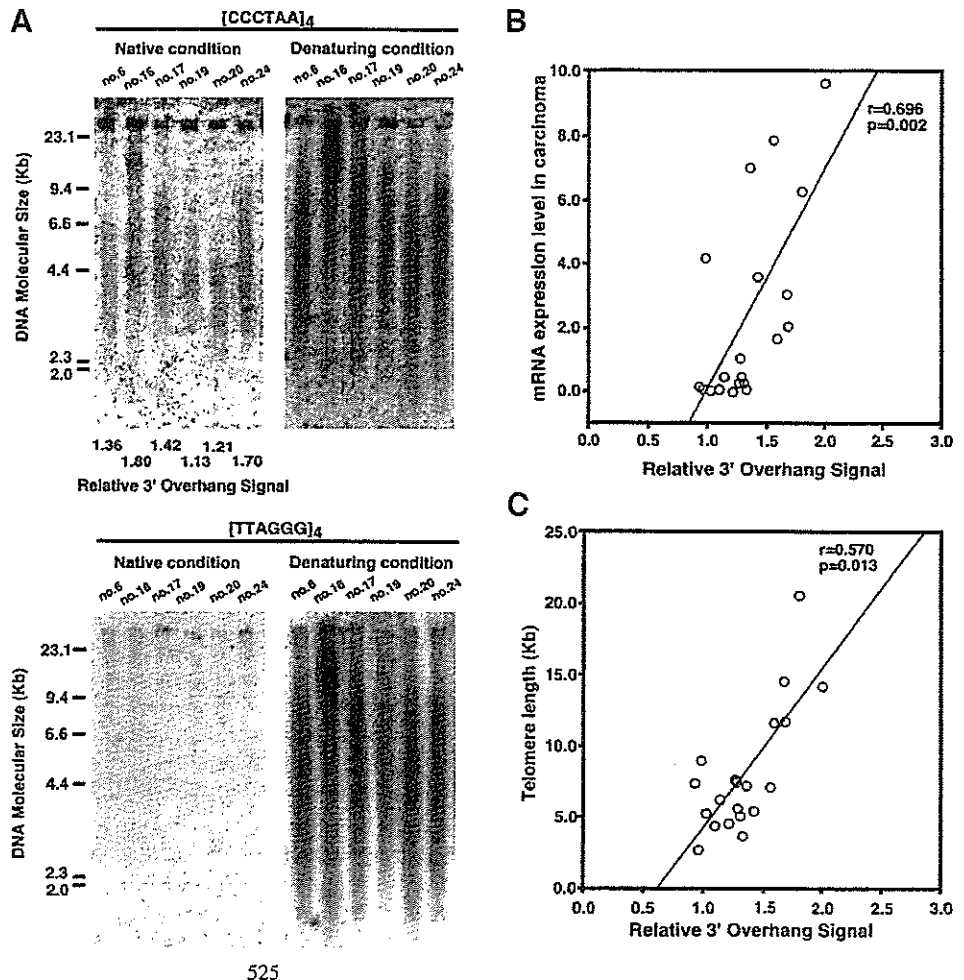
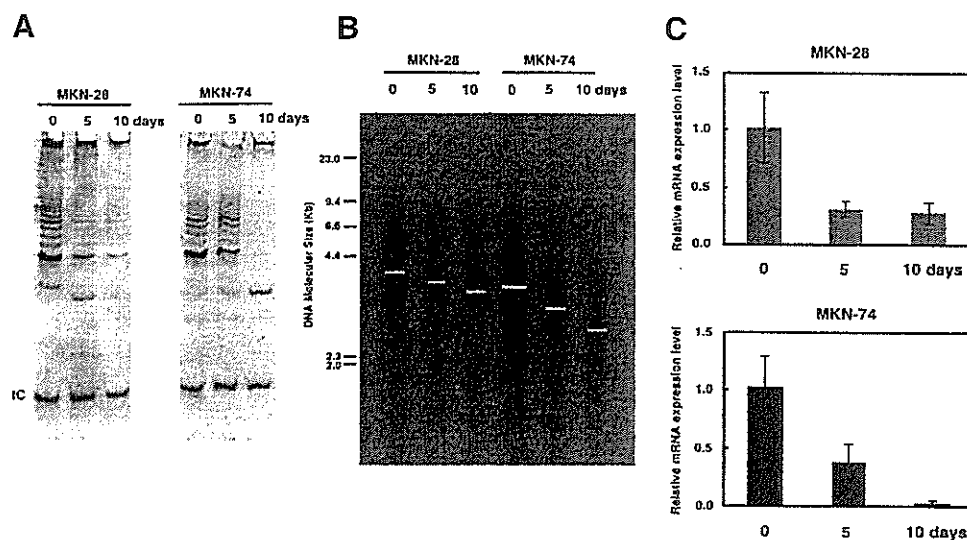


Fig. 3. *POT1* expression levels in relation to telomere shortening. **A**, reduced telomerase activity in MKN-28 and MKN-74 cells is observed after 5 and 10 days' treatment with azidothymidine (AZT). IC = internal control (36 bp). **B**, Telomere shortening is observed in MKN-28 and MKN-74 cells after 5 and 10 days' treatment with AZT. **C**, quantitative reverse-transcription-PCR analysis showed reduced *POT1* expression in MKN-28 and MKN-74 cells treated with AZT. *POT1* expression levels are the mean  $\pm$  SD and relative to levels in nontreated cells.



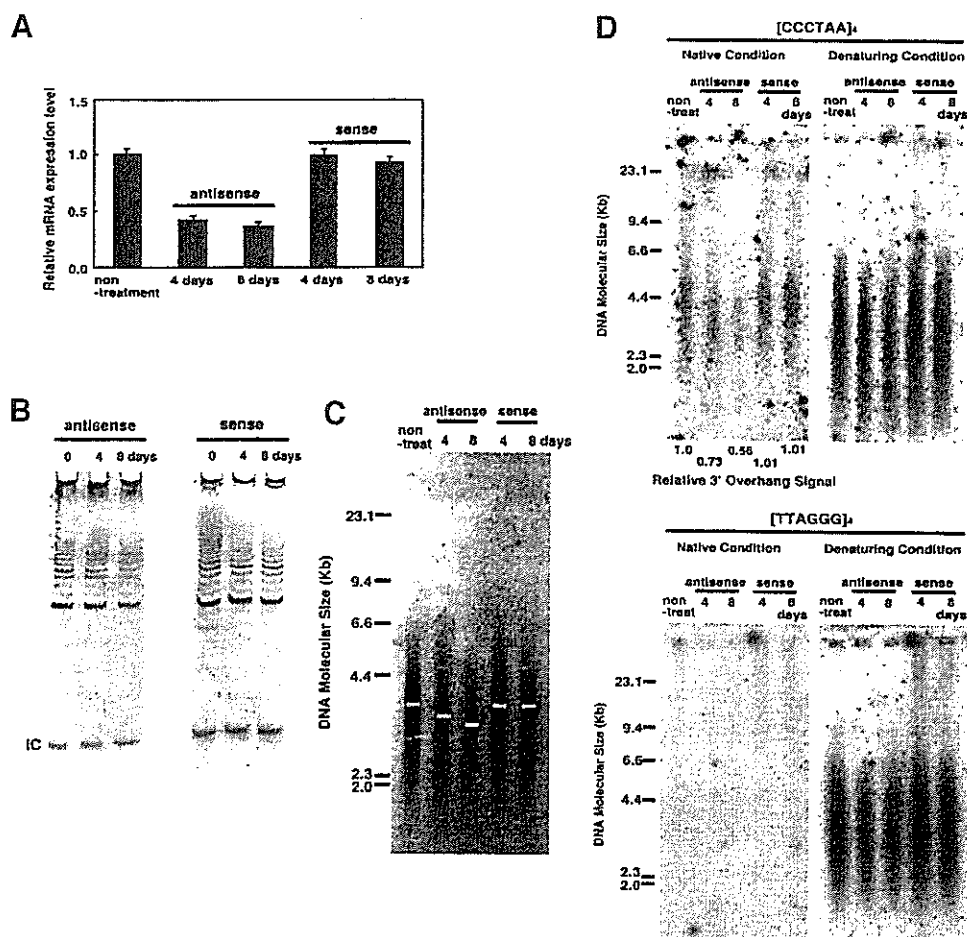
5 days and 26% after 10 days. And expression of *POT1* in AZT-treated MKN-74 cells was 36% of that in nontreated cells after 5 days and 1% after 10 days.

**Inhibition of *POT1* Induces Telomere Shortening.** For additional analysis, we examined MKN-28 cells treated with *POT1* antisense oligonucleotides. Decreased *POT1* expression was confirmed by quantitative RT-PCR in MKN-28 cells after treatment with antisense oligonucleotides (Fig. 4A). Expression of *POT1* in antisense oligonucleotide-treated MKN-28 cells was 40% of nontreated cells after 4 days and 34% after 8 days. Treatment with *POT1* antisense

oligonucleotides resulted in telomerase inhibition (by 58% after 4 days and 83% after 8 days; Fig. 4B) and telomere shortening (from 3.8 to 3.3 Kb after 4 days and to 3.0 Kb after 8 days; Fig. 4C). Treatment with sense oligonucleotides did not produce any alterations in *POT1* expression levels, telomerase activity, or telomere length.

**Inhibition of *POT1* Reduces 3' Telomeric Overhang Signals.** To test whether *POT1* expression levels are associated with 3' overhang signals, 3' telomeric overhang signals were examined by in-gel hybridization in MKN-28 cells treated with *POT1* antisense oligonucleotides. A reduction in 3' overhang signals was found in antisense

Fig. 4. Telomere shortening, telomerase inhibition and the reduction of 3' telomeric overhang signals in association with reduced expression of *POT1* in antisense oligonucleotides-treated MKN-28 cells. **A**, reduction of *POT1* expression was confirmed in MKN-28 cells after antisense oligonucleotide treatment for 4 and 8 days. **B**, reduced telomerase activity was detected in antisense oligonucleotides-treated MKN-28 cells, whereas telomerase activity was not changed in sense oligonucleotides-treated MKN-28 cells. **C**, telomere shortening was detected in MKN-28 cells treated with antisense oligonucleotides. **D**, inhibition of Pot1 reduced 3' telomeric overhang signals. The top left panel shows native gel probed with [CCCTAA]<sub>n</sub>, and the top right panel shows denatured gel probed with [CCCTAA]<sub>n</sub>. The bottom left panel shows native gel probed with [TTAGGG]<sub>n</sub>, and the bottom right panel shows denatured gel probed with [TTAGGG]<sub>n</sub>. Signals were expressed relative to the signal in the nontreated MKN-28 gastric cancer cells and normalized to the amount of DNA (10  $\mu$ g) loaded based on denatured gels.



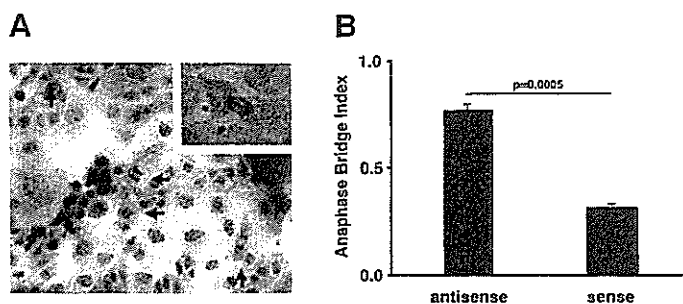


Fig. 5. Inhibition of Pot1 increases the incident of anaphase bridge. A, photomicrograph of typical anaphase bridge (arrows and inset) in MKN-28 treated with *POT1* antisense oligonucleotides H&E-stained section. (magnification,  $\times 400$ ; inset magnification,  $\times 1000$ ). B, inhibition of Pot1 by antisense oligonucleotides increases the number of anaphase bridge in MKN-28 gastric cancer cells.

oligonucleotide-treated cells (to 73% after 4 days and to 56% after 8 days; Fig. 4D). Signals in sense oligonucleotide-treated cells were almost the same as signals in nontreated cells (101% after both 4 and 8 days).

**Inhibition of *POT1* Expression Increases the Frequency of Anaphase Bridges.** To examine association between *POT1* expression levels and telomere dysfunction, we determined the ABI in the 51 GC tissues. No significant association was found between *POT1* expression levels and the ABI. Moreover, the ABI did not correlate with telomere length or 3' telomeric overhang signals (data not shown). We then treated MKN-28 cells with *POT1* antisense and sense oligonucleotides for 8 days and determined the ABI. Treatment with *POT1* antisense increased the ABI in MKN-28 cells to about twice that of sense-treated cells (0.76 for antisense treatment and 0.31 for sense treatment;  $P = 0.0005$ , unpaired *t* test; Fig. 5, A and B).

## DISCUSSION

Pot1 is thought to have two functions. One is mediating recruitment of telomerase, and the other is protecting the 3' telomeric overhang from degradation and DNA repair activities (13, 16–18). We studied *POT1* mRNA expression in GC tissues with respect to both functions. We showed expression levels of *POT1* in the GC tissues relative to levels in nonneoplastic mucosae to be significantly associated with tumor stage and that up-regulation of *POT1* occurs preferentially in late-stage GC. Pot1 is thought to protect telomeres (13). In fact, inhibition of *POT1* by antisense oligonucleotides led to an increase in the frequency of anaphase bridge in MKN-28 cells. Thus, inhibition of Pot1 is associated with telomere dysfunction. Previous studies in a mouse model revealed that severe telomere dysfunction impaired tumor progression (26–31). Severe telomere dysfunction is shown to be reduced in advanced tumors that survive after crisis (26, 32, 33). Thus, up-regulated *POT1* may participate in protection of the telomere ends in late-stage GC. In addition, we found *POT1* mRNA expression levels to be associated with telomere length, as well as 3' telomeric overhang signals in GC tissues. However, we did not find significant association between telomere length or 3' telomeric overhang signals and tumor stage (data not shown). High-level *POT1* expression, as well as telomerase activity, may be required for maintenance of telomere function.

Telomere dysfunction appears to occur in cancer precursor lesions and increase the frequency of genetically initiated neoplasms (26, 30, 31, 34–39); therefore, in early-stage GC after neoplasm initiation, down-regulation of *POT1* may occur preferentially. We showed that down-regulation of *POT1* was observed preferentially in low T grade cancers, which might also reflect telomere dysfunction in early-stage GC. Approximately half of our GC patients (21 of 51) showed no

changes in the expression level of *POT1*, perhaps because telomere dysfunction is circumvented by chromosomal rearrangement such as in decentric and ring chromosomes in these patients.

The ABI did not correlate with *POT1* expression levels, telomere length, or 3' telomeric overhang signals. Anaphase bridges are chromatin bridges that are not resolved after anaphase, and they result in breakage-fusion-bridge cycles that produce rapid and widespread changes in the gene (40–46). Anaphase bridges are a hallmark of telomere dysfunction (26) but form not only as a result of defects in telomere structure or length (6, 34) but also as a result of defects in DNA replication (47), recombinations (48), or translocations that introduce a second centromere into the chromosome (46, 49). Therefore, we could not show significant association between ABI and *POT1* expression levels, telomere length, or 3' telomeric overhang signals.

It was reported recently that the 3' telomeric overhang is shortened at senescence and that progressive overhang loss occurred in cells that avoided senescence through inactivation of p53 and Rb (50). Evidence indicates that 3' telomeric overhang shortening is the result of continuous cell division and that it is associated with telomere shortening. We showed telomere length to be associated with 3' telomeric overhang signals, consistent with previously reported findings (50).

To confirm the association between *POT1* expression levels and telomere length, we measured telomere length in AZT-treated GC cells and showed reduced *POT1* expression as well as telomere shortening. Loayza *et al.* (51) also reported the amount of Pot1 to be correlated with telomere length. Our data support their findings. However, we cannot fully rule out the possibility that the down-regulation of *POT1* may have been because of a direct effect of AZT or other factors. We examined association between *POT1* expression levels and telomere length, 3' telomeric overhangs, and the frequency of anaphase bridges using GC cells treated with *POT1* antisense oligonucleotides. The inhibition of *POT1* by antisense oligonucleotides was found to shorten the telomere, reduce the 3' overhang signals, and increase the frequency of anaphase bridges. Colgin *et al.* (52) reported that overexpression of *POT1* led to telomere elongation. In yeast, Pot1-like protein Cdc13 recruits telomerase to the 3' telomeric overhang (14); thus, inhibition of *POT1* may lead to telomere shortening through inhibition of recruitment of telomerase to the 3' telomeric overhang. Furthermore, our study showed that inhibition of telomerase activity occurred via *POT1* antisense oligonucleotides. We are unable to explain this phenomenon at the present. However, inhibition of telomerase activity by *POT1* antisense oligonucleotides may participate partly in telomere shortening. We examined the viability of antisense-treated MKN-28 cells (4- and 8-day treatments) by 3-(4,5-dimethylthiazol-2-yl)-2,5-diphenyltetrazolium bromide assay and observed no change in the viability of treated cells compared with nontreated cells (data not shown). Thus, it seems there is no association between telomerase inhibition and decreased viability of cells. We found inhibition of *POT1* by antisense oligonucleotides to reduce 3' overhang signals. Therefore, it is possible that *POT1* expression levels may generally depend on the size of the 3' telomeric overhang. However, it remains a possibility that the reduction of 3' overhang signals may be because of end-to-end fusion. Indeed, inhibition of *POT1* led to an increase in the frequency of anaphase bridges. In this study, no signal was present at the position of the larger terminal fragments representing the fused telomeres (53). Therefore, at least some of the loss of 3' overhangs in GC cells must have taken place on unfused chromosome ends, and end-to-end fusion may have little effect on 3' overhang signals.

Loayza *et al.* (51) observed telomere elongation using Pot1 mutant lacking the oligosaccharide/oligonucleotide-binding (OB) fold required for DNA binding. We are unable to fully explain the discrep-



ancy between the Loayza *et al.* (51) findings and those of Colgin *et al.* (52) along with ours. There are several possible explanations: we and Colgin *et al.* (52) altered whole expression levels of wild-type *POT1* with antisense oligonucleotides and expression vectors (52); thus, the discrepancy may be because of methodological differences. We did not perform any mutation analysis in the oligosaccharide/oligonucleotide-binding (OB) fold of Pot1 in the present study. This should be done in further study. Although telomere length may be regulated by the interaction between Pot1 and TRF1 complex, we did not examine TRF1 expression status in the present study. In yeast, the interaction between Cdc13 and telomerase has been previously described (14), but in human cells, the interaction between Pot1 and telomerase has not been examined. We presume that such investigation is most essential to understanding the function of Pot1.

Adequate telomere length, telomerase activity, and T-loop formation are required for maintenance of telomere function, and when only one mechanistic factor is compromised such as in a lack of functional telomerase or telomere shortening, the other components of the capping system can compensate (16). The association we observed between telomere length and telomerase activity indicates that Pot1 may play an important role in the maintenance of telomere function. Telomere dysfunction leads to genetic instability at the chromosome ends, and such instability is associated with the initiation of carcinogenesis (26, 30, 31, 34–39). We consider reduced levels of *POT1* expression to reflect telomere dysfunction and that they may serve as a useful screening tool for identifying individuals at greatest risk of carcinogenesis. Additional studies are needed to establish Pot1 as a clinical indicator of cancer risk.

**ACKNOWLEDGMENTS**

We thank Masayoshi Takatani and Mutsumi Ueda for their excellent technical assistance and advice, and Dr. Keiko Hiyama, Department of Translational Cancer Research, Research Institute for Radiation Biology and Medicine, Hiroshima University, for helpful discussions.

**REFERENCES**

1. Makarov, V. L., Hirose, Y., and Langmore, J. P. Long G tails at both ends of human chromosomes suggest a C strand degradation mechanism for telomere shortening. *Cell*, **88**: 657–666, 1997.
2. McElligott, R., and Wellinger, R. J. The terminal DNA structure of mammalian chromosomes. *EMBO J.*, **16**: 3705–3714, 1997.
3. Wright, W. E., Tesmer, V. M., Liao, M. L., and Shay, J. W. Normal human telomeres are not late replicating. *Exp. Cell Res.*, **251**: 492–499, 1999.
4. Hanish, J. P., Yanowitz, J. L., and de Lange, T. Stringent sequence requirements for the formation of human telomeres. *Proc. Natl. Acad. Sci. USA*, **91**: 8861–8865, 1994.
5. Allsopp, R. C., and Harley, C. B. Evidence for a critical telomere length in senescent human fibroblasts. *Exp. Cell Res.*, **219**: 130–136, 1995.
6. Harley, C. B., and Villeponteau, B. Telomeres and telomerase in aging and cancer. *Curr. Opin. Genet. Dev.*, **5**: 249–255, 1995.
7. Romero, D. P., and Blackburn, E. H. A conserved secondary structure for telomerase RNA. *Cell*, **67**: 343–353, 1991.
8. Lingner, J., Cooper, J. P., and Cech, T. R. Telomerase and DNA end replication: no longer a lagging strand problem? *Science (Wash. DC)*, **269**: 1533–1534, 1995.
9. Linger, J., Hughes, T. R., Shevchenko, A., Mann, M., Lundblad, V., and Cech, T. R. Reverse transcriptase motifs in the catalytic subunit of telomerase. *Science (Wash. DC)*, **277**: 955–959, 1997.
10. Prowse, K. R., and Greider, C. W. Developmental and tissue-specific regulation of mouse telomerase and telomere length. *Proc. Natl. Acad. Sci. USA*, **92**: 4818–4822, 1995.
11. Tahara, H., Kuniyasu, H., Yokosaki, H., Yasui, W., Shay, J. W., Ide, T., and Tahara, E. Telomerase activity in preneoplastic and neoplastic gastric and colorectal lesions. *Clin. Cancer Res.*, **1**: 1245–1251, 1995.
12. Yasui, W., Tahara, E., Tahara, H., Fujimoto, J., Naka, K., Nakayama, J., Ishikawa, F., Ide, T., and Tahara, E. Immunohistochemical detection of human telomerase reverse transcriptase in normal mucosa and precancerous lesion of the stomach. *Jpn. J. Cancer Res.*, **90**: 589–595, 1999.
13. Baumann, P., and Cech, T. R. Pot1, the putative telomere end-binding protein in fission yeast and humans. *Science (Wash. DC)*, **292**: 1171–1175, 2001.
14. Evans, S. K., and Lundblad, V. Est1 and Cdc13 as comediators of telomerase access. *Science (Wash. DC)*, **286**: 117–120, 1999.

15. Nugent, C. I., Hughes, T. R., Lue, N. F., and Lundblad, V. Cdc13p: a single-strand telomeric DNA-binding protein with a dual role in yeast telomere maintenance. *Science (Wash. DC)*, **274**: 249–252, 1996.
16. Blackburn, E. H. Switching and signaling at the telomere. *Cell*, **106**: 661–673, 2001.
17. Baumann, P., Podell, E., and Cech, T. R. Human Pot1 (protection of telomeres) protein: cytolocalization, gene structure, and alternative splicing. *Mol. Cell. Biol.*, **22**: 8079–8087, 2002.
18. Lei, M., Baumann, P., and Cech, T. R. Cooperative binding of single-stranded telomeric DNA by the Pot1 protein of *Schizosaccharomyces pombe*. *Biochemistry*, **41**: 14560–14568, 2002.
19. Strahl, C., and Blackburn, E. H. The effects of nucleoside analogs on telomerase and telomeres in *Tetrahymena*. *Nucleic Acids Res.*, **22**: 893–900, 1994.
20. Strahl, C., and Blackburn, E. H. Effect of reverse transcriptase inhibitors on telomere length and telomerase activity in two immortalized human cell lines. *Mol. Cell. Biol.*, **16**: 53–65, 1996.
21. Rha, S. Y., Izbicka, E., Lawrence, R., Davidson, K., Sun, D., Moyer, M. P., Roodman, G. D., Hurlley, L., and Von Hoff, D. Effect of telomere and telomerase interactive agents on human tumor and normal cell lines. *Clin. Cancer Res.*, **6**: 987–989, 2000.
22. Mo, Y., Gan, Y., Song, S., Johnston, J., Xiao, X., Wientjes, M. G., and Au, J. L. Simultaneous targeting of telomeres and telomerase as a cancer therapeutic approach. *Cancer Res.*, **63**: 579–585, 2003.
23. Lauren, P. The two histological main types of gastric carcinoma. Diffuse and so-called intestinal type carcinoma: an attempt at histological classification. *Acta Pathol. Microbiol. Scand.*, **64**: 31–49, 1965.
24. Sobin, L. H., and Wittekind, C. H. (eds.). *TNM Classification of Malignant Tumors, Digestive System Tumours*, Ed. 5, pp. 59–62. New York: Wiley-Liss, Inc., 1997.
25. Dionne, I., and Wellinger, R. J. Cell cycle-regulated generation of single-stranded G-rich DNA in the absence of telomerase. *Proc. Natl. Acad. Sci. USA*, **93**: 13902–13907, 1996.
26. Rudolph, K. L., Millard, M., Bosenberg, M. W., and DePinho, R. A. Telomere dysfunction and evolution of intestinal carcinoma in mice and humans. *Nat. Genet.*, **28**: 155–159, 2001.
27. Greenberg, R. A., Chin, L., Femino, A., Lee, K. H., Gottlieb, G. J., Singer, R. H., Greider, C. W., and DePinho, R. A. Short dysfunctional telomeres impair tumorigenesis in the *INK4a<sup>Δ2/3</sup>* cancer-prone mouse. *Cell*, **97**: 515–525, 1999.
28. Gonzalez-Suarez, E., Samper, E., Flores, J. M., and Blasco, M. A. Telomerase-deficient mice with short telomeres are resistant to skin tumorigenesis. *Nat. Genet.*, **26**: 114–117, 2000.
29. Farazi, P. A., Glickman, J., Jiang, S., Yu, A., Rudolph, K. L., and DePinho, R. A. Differential impact of telomere dysfunction on initiation and progression of hepatocellular carcinoma. *Cancer Res.*, **63**: 5021–5027, 2003.
30. Maser, R. S., and DePinho, R. A. Connecting chromosomes, crisis, and cancer. *Science (Wash. DC)*, **297**: 565–569, 2002.
31. Artandi, S. E., and DePinho, R. A. Mice without telomerase: what can they teach us about human cancer? *Nat. Med.*, **6**: 852–855, 2000.
32. Gordon, K. E., Ireland, H., Roberts, M., Steeghs, K., McCaul, J. A., MacDonald, D. G., and Parkinson, E. K. High levels of telomere dysfunction bestow a selective disadvantage during the progression of human oral squamous cell carcinoma. *Cancer Res.*, **63**: 458–467, 2003.
33. Counter, C. M., Avilion, A. A., LeFeuvre, C. E., Stewart, N. G., Harley, C. B., and Bacchetti, S. Telomere shortening associated with chromosome instability is arrested in immortal cells which express telomerase activity. *EMBO J.*, **11**: 1921–1929, 1992.
34. O'Sullivan, J. N., Bronner, M. P., Brentnall, T. A., Finley, J. C., Shen, W. T., Emerson, S., Emond, M. J., Gollakoti, K. A., Moskovitz, A. H., Crispin, D. A., Potter, J. D., and Rabinovitch, P. S. Chromosomal instability in ulcerative colitis is related to telomere shortening. *Nat. Genet.*, **32**: 280–284, 2002.
35. Meeker, A. K., Hicks, J. L., Platz, E. A., March, G. E., Bennett, C. J., Delannoy, M. J., and De Marzo, A. M. Telomere shortening is an early somatic DNA alteration in human prostate tumorigenesis. *Cancer Res.*, **62**: 6405–6409, 2002.
36. Van Heek, N. T., Meeker, A. K., Kern, S. E., Yeo, C. J., Lillemoe, K. D., Cameron, J. L., Offerhaus, G. L., Hicks, J. L., Wilentz, R. E., Goggins, M. G., De Marzo, A. M., Hruban, R. H., and Maitra, A. Telomere shortening is nearly universal in pancreatic intraepithelial neoplasia. *Am. J. Pathol.*, **161**: 1541–1547, 2002.
37. Chin, L., Artandi, S. E., Shen, Q., Tam, A., Lee, S. L., Gottlieb, G. J., Greider, C. W., and DePinho, R. A. p53 deficiency rescues the adverse effects of telomere loss and cooperates with telomere dysfunction to accelerate carcinogenesis. *Cell*, **97**: 527–538, 1999.
38. Artandi, S. E., Chang, S., Lee, S. L., Alson, S., Gottlieb, G. J., Chin, L., and DePinho, R. A. Telomere dysfunction promotes non-reciprocal translocations and epithelial cancers in mice. *Nature (Lond.)*, **406**: 641–645, 2000.
39. DePinho, R. A. The age of cancer. *Nature (Lond.)*, **408**: 248–254, 2000.
40. McClintock, B. The production of homozygous deficient tissues with mutant characteristics by means of the aberrant behavior of ring-shaped chromosomes. *Genetics*, **23**: 315–376, 1938.
41. McClintock, B. The stability of broken ends of chromosomes in *Zea mays*. *Genetics*, **26**: 234–282, 1940.
42. Gisselsson, D., Bjork, J., Hoglund, M., Mertens, F., Dai Cin, P., Akerman, M., and Mandahl, N. Abnormal nuclear shape in solid tumors reflects mitotic instability. *Am. J. Pathol.*, **158**: 199–206, 2001.
43. Gisselsson, D., Pettersson, L., Hoglund, M., Heidenblad, M., Gorunova, L., Wiegant, J., Mertens, F., Dai Cin, P., Mitelman, F., and Mandahl, N. Chromosomal breakage-fusion-bridge events cause genetic intratumor heterogeneity. *Proc. Natl. Acad. Sci. USA*, **97**: 5357–5362, 2000.



44. Montgomery, E., Wilentz, R. E., Argani, P., Fisher, C., Hruban, R. H., Kern, S. E., and Lengauer, C. Analysis of anaphase figures in routine histologic sections distinguishes chromosomally unstable from chromosomally stable malignancies. *Cancer Biol. Ther.*, 2: 243–252, 2003.
45. Gisselsson, D., Jonson, T., Petersen, A., Strombeck, B., Dal Cin, P., Hoglund, M., Mitelman, F., Metens, F., and Mandahl, N. Telomere dysfunction triggers extensive DNA fragmentation and evolution of complex chromosome abnormalities in human malignant tumors. *Proc. Natl. Acad. Sci. USA*, 98: 12683–12688, 2001.
46. Saunders, W. S., Shuster, M., Huang, X., Gharaibeh, B., Enyenihi, A. H., Petersen, I., and Gollin, S. M. Chromosomal instability and cytoskeletal defects in oral cancer cells. *Proc. Natl. Acad. Sci. USA*, 97: 303–308, 2000.
47. Poupon, M. F., Smith, K. A., Chernova, O. B., Gilbert, C., and Stark, G. R. Inefficient growth arrest in response to dNTP starvation stimulates gene amplification through bridge-breakage-fusion cycles. *Mol. Biol. Cell*, 7: 345–354, 1996.
48. Smith, K. A., Gorman, P. A., Stark, M. B., Groves, R. P., and Stark, G. R. Distinctive chromosomal structures are formed very early in the amplification of *CAD* genes in Syrian hamster cells. *Cell*, 63: 1219–1227, 1990.
49. Hastie, N. D., and Allshire, R. C. Human telomeres: fusion and interstitial sites. *Trends Genet.*, 5: 326–331, 1989.
50. Stewart, S. A., Ben-Porath, I., Carey, V. J., O'Connor, B. F., Hahn, W. C., and Weinberg, R. A. Erosion of the telomeric single-strand overhang at replicative senescence. *Nat. Genet.*, 33: 492–496, 2003.
51. Loayza, D., and de Lange, T. POT1 as a terminal transducer of TRF1 telomere length control. *Nature (Lond.)*, 423: 1013–1018, 2003.
52. Colgin, L. M., Baran, K., Baumann, P., Cech, T. R., and Reddel, R. R. Human POT1 facilitates telomere elongation by telomerase. *Curr. Biol.*, 13: 942–946, 2003.
53. van Steensel, B., Smogorzewska, A., and de Lange, T. TRF2 protects human telomeres from end-to-end fusions. *Cell*, 92: 401–413, 1998.

# Improving the efficiency of nested case-control studies of interaction by selecting controls using counter matching on exposure

John B Cologne,<sup>1</sup> Gerald B Sharp,<sup>2</sup> Kazuo Neriishi,<sup>3</sup> Pia K Verkasalo,<sup>5</sup> Charles E Land<sup>6</sup> and Kei Nakachi<sup>4</sup>

Accepted 17 December 2003

**Background** Studies of the effect of exposure to a risk factor measured in an entire cohort may be augmented by nested case-control subsets to investigate confounding or effect modification by additional factors not practically assessed on all cohort members. We compared three control-selection strategies—matching on exposure, counter matching on exposure, and random sampling—to determine which was most efficient in a situation where exposure is a known, continuous variable and high doses are rare.

**Methods** We estimated the power to detect interaction using four control-to-case ratios (1:1, 2:1, 4:1, and 8:1) in a planned case-control study of the joint effect of atomic bomb radiation exposure and serum oestradiol levels on breast cancer. Radiation dose is measured in the entire cohort, but because neither serum oestradiol level nor the true degree of interaction was known, we simulated values of oestradiol and hypothetical levels of oestradiol–radiation interaction.

**Results** Compared with random sampling, power to detect interaction was similarly higher with either matching or counter matching with two or more controls.

**Conclusions** Because counter matching is generally at least as efficient as random sampling, whereas matching on exposure can result in loss of efficiency and precludes estimation of exposure risk, we recommend counter matching for selecting controls in nested case-control studies of the joint effects of multiple risk factors when one is previously measured in the full cohort.

**Keywords** Nested case-control studies, probability sample, matching, counter matching, breast cancer, radiation effects

In cohort studies aimed at investigating the effects of already measured risk factors—such as radiation exposure in the survivors of the atomic bombings of Hiroshima and Nagasaki, Japan—nested case-control studies may be conducted to analyse the effects of additional factors that cannot be assessed

practically in the entire cohort. The purpose might be to study the effects of potential confounders or effect-modifying factors on the exposure risk. If the exposure is rare or has a skewed distribution, ignoring it in selecting controls can lead to a loss of statistical efficiency, so exposure-based methods of control selection might be considered.

As an example, although radiation and oestradiol are both strong risk factors for breast cancer, only radiation dose is known for atomic bomb survivors. The relative risk of early-onset breast cancer (diagnosis under age 35) for 1 Sv of radiation is 14 among women irradiated by the atomic bombs before age 20; the overall relative risk of breast cancer ranges from 2.3 to 3.4 among all women exposed under the age of 40.<sup>1</sup> Key, Verkasalo, and Banks showed that serum oestradiol is

Departments of <sup>1</sup>Statistics, <sup>2</sup>Epidemiology, <sup>3</sup>Clinical Studies, and <sup>4</sup>Radiobiology/Molecular Epidemiology, Radiation Effects Research Foundation, Hiroshima, Japan.

<sup>5</sup>Unit of Environmental Epidemiology, National Public Health Institute, Finland.

<sup>6</sup>Radiation Epidemiology Branch, National Cancer Institute, US.

Correspondence: John B Cologne, Department of Statistics, Radiation Effects Research Foundation, 5-2 Hijiyama Park, Minami-ku, Hiroshima 732-0815, Japan. E-mail: cologne@rerf.or.jp

positively associated with risk of breast cancer, with risks being about twice as high for postmenopausal women with high, as opposed to low, serum oestradiol concentrations.<sup>2</sup> Little is known, however, about oestradiol levels and the risk of pre-menopausal breast cancer. Furthermore, the joint effect of radiation and oestradiol has not been studied, although Land *et al.*<sup>3</sup> demonstrated interactions between radiation and breast cancer risk factors that may be related to constitutional hormone levels. At the Radiation Effects Research Foundation (RERF), we are conducting a study of radiation and oestradiol as joint risk factors for pre-menopausal breast cancer using stored sera obtained from atomic bomb survivors who participated in biennial clinical examinations conducted for RERF's Adult Health Study. Oestradiol, which is expensive to assay and requires sera, for which supplies are limited, will be measured in all cases but only a subset of controls. This raises the issue of how best to select controls to provide maximum statistical efficiency.

Selecting controls by individually matching them to cases on radiation exposure can improve statistical efficiency for testing interaction with another factor.<sup>4</sup> If there is evidence of interaction or possible confounding in the case-control sample, a logical next step in the analysis would be to examine how exposure risk estimates vary with the level of the other factor. Matching on exposure allows studying the effect of confounder/effect-modifier *per se* but precludes studying its effect on the exposure risk without additional information, such as comes from the cohort.<sup>3</sup> An alternative to matching is weighted sampling of controls using counter-matching, where controls are selected to fill exposure strata not occupied by the case.<sup>5-8</sup> Counter matching also allows estimation of the exposure risk, and the efficiency for studying both confounding and effect modification can be improved relative to random sampling of controls.<sup>9</sup> Furthermore, counter matching allows the investigator to fix the number of controls in advance and is easily implemented with prospective, risk-set based selection. Many of the references on these designs provide justification and intuitive explanation as to why exposure-based sampling is efficient.

Counter matching has been shown to generate better efficiency for testing interaction than matching over a wide range of exposure risks and degrees of correlation between exposure and another risk factor when both are dichotomous,<sup>8</sup> but comparisons have not been made for continuous risk factors, such as radiation dose and oestradiol. The proposed breast cancer study provides a basis for making that comparison in the case of a rare exposure that may interact positively with an additional factor, the situation in which matching achieves the greatest gain in efficiency.<sup>4</sup> Our objective was to assess the extent to which matching and counter matching impact statistical power for detecting interaction relative to random control selection.

## Subjects and Methods

### Study design

We are conducting a nested case-control study of pre-menopausal breast cancer, radiation exposure, and serum oestradiol levels using all currently available cases.<sup>10</sup> Radiation doses are known, but oestradiol is to be measured in the

case-control subset using stored sera. Day of menstrual cycle at the time of serum collection is not known; therefore it was decided to use the average of two measurements on serum specimens collected on different occasions. There were 80 cases of pre-menopausal breast cancer and 5644 cancer-free women with stored serum. Radiation doses were calculated according to Dosimetry System 1986 (DS86).<sup>11</sup> Radiation doses to the breast were calculated in Sievert (Sv), combining gamma and neutron components with a relative weight of 10 for neutrons.

To assess the power of the study for detecting interaction, we simulated oestradiol levels and their interaction with radiation. We then calculated the resulting power using one, two, four, or eight controls selected from case risk-sets using three approaches: (1) random sampling, (2) matching as closely as possible on radiation exposure, or (3) counter matching on radiation exposure.

Selecting controls by random sampling is simple. Within risk sets defined by age, date, and availability of stored serum, controls are selected at random, without regard for exposure status. Matching on radiation exposure is also straightforward; within each risk set, the potential controls whose exposure values are closest to the case's exposure are selected. Note, however, that matching on exposure in addition to matching on other factors can be more complicated.<sup>12</sup> If there are more tied values among the potential controls than the number needed, the controls are selected at random from among the tied subjects.

With counter matching, exposure strata are defined based on the number of controls to be selected per case and on the distribution of exposure among the cases. In each risk set one control is selected from each of the exposure strata not occupied by the case. In the study described here, there were many people with dose zero; we therefore defined the lowest exposure category to be zero. The other categories were determined by the appropriate percentiles of the distribution of exposure values among the exposed cases. For example, with eight controls per case there were nine exposure strata: zero plus eighths defined by octiles of the case exposure values (cutpoints: 0.14, 0.45, 0.66, 0.79, 1.15, 1.50, and 2.04 Sv; Supplementary Material: Distribution of Radiation Doses). With four controls per case there were five strata: zero plus fourths defined by quartiles of the case exposures (cutpoints: 0.45, 0.79, and 1.50 Sv; Figure 1).

### Simulation of serum oestradiol levels and interaction with radiation

Oestradiol values were computer generated to have overall mean and variance equal to those from a previous study performed in the same cohort.<sup>13</sup> Because there was no information about day of menstrual cycle on which serum was collected, we accounted for day-to-day variation by mimicking random sampling from the menstrual cycle using data for British women from Verkasalo and her associates.<sup>14</sup> First, a random integer representing day of cycle was obtained using a uniform random number generator. Then, a random  $\log_{10}$ -oestradiol value was obtained by generating a random Normal variable with mean and variance equal to those for the same cycle day among the British study group. Finally, the resulting values were adjusted to have overall (not day-specific) mean and variance equal to those found in the previous atomic bomb

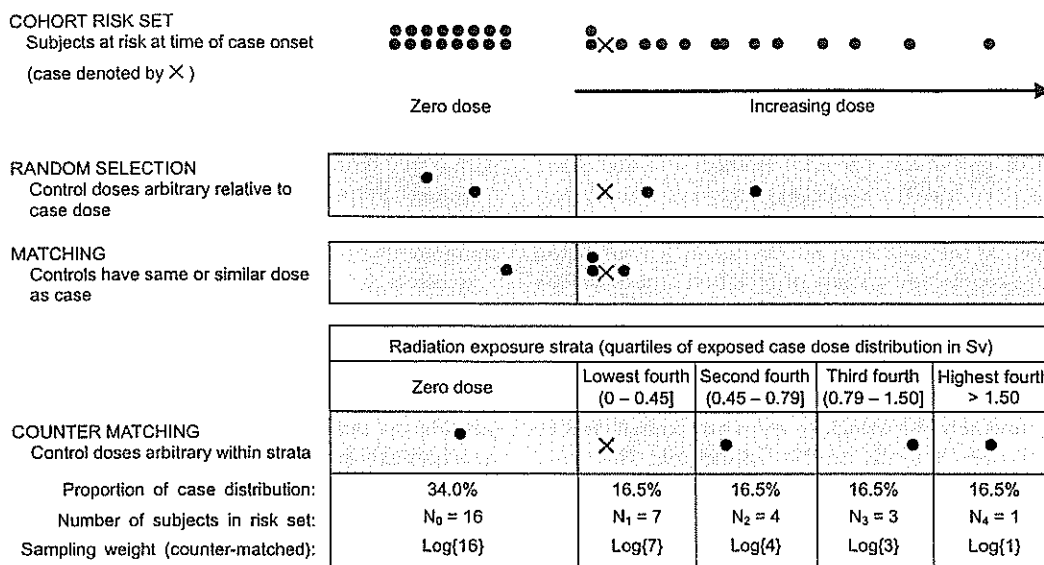


**Figure 1** Illustration of control-selection strategies with four controls per case. The case exposure value (X) in this illustration is close to zero and in the lowest of the fourths derived from quartiles among non-zero-dose cases. With random sampling, controls would be selected randomly without regard to their dose. With matching, the four controls with doses closest to that of the case would be selected. With counter matching, one control would be selected randomly from each of the non-case strata (the remaining three exposure fourths and the zero-dose stratum)

survivor study. This adjustment was made separately for cases and controls. The simulated values were standardized to produce a log odds ratio of  $\phi_A = 0.359$ , the result obtained with an average  $\log_{10}$ -oestradiol difference of 7% between cases and controls in the previous study, where controls were matched to cases on radiation dose. This corresponds to odds of disease of 1.43 for a 1.41-fold higher oestradiol level. For each subject we used the average of two simulated oestradiol values from arbitrary cycle days to reduce the error due to lack of knowledge of cycle day on which the serum was collected.

Because radiation dose and case status were already known in the cohort, we simulated the interaction by adjusting the mean of the Normal distribution from which case  $\log_{10}$ -oestradiol values were generated so that the average case-control mean difference in  $\log_{10}$ -oestradiol level increased linearly with radiation dose, while  $\log_{10}$ -oestradiol values among the controls were generated independently of radiation dose. The dose-dependent case  $\log_{10}$ -oestradiol means were calculated to produce log odds ratios (OR) according to the following model:

$$\phi(d) = \phi_A \times f(d) = \phi_A \times \left[ 1 + \gamma \left( \frac{d - 0.75}{0.75} \right) \right]$$

so that the log OR is  $\phi_A$  at a dose of 0.75 Sv, close to the average dose among the cases. Three levels of interaction were selected to produce low, moderate, and high power of detection in the full cohort. These were simulated by setting  $\gamma$  so that, with a doubling of dose to 1.5 Sv, the relative changes in the log OR for  $\log_{10}$ -oestradiol with interaction were 0.5 (low degree of interaction), 0.75 (moderate degree of interaction), or 1.0 (high degree of interaction); Figure 2. The low degree of interaction results in a log OR of  $0.5\phi$  (OR = 1.20) at 0 Sv and a log OR of  $1.5\phi$  (OR = 1.71) at twice the median dose (1.5 Sv). The moderate degree of interaction results in corresponding log OR of  $0.25\phi$  and  $1.75\phi$  (OR = 1.09 and 1.87). The high degree

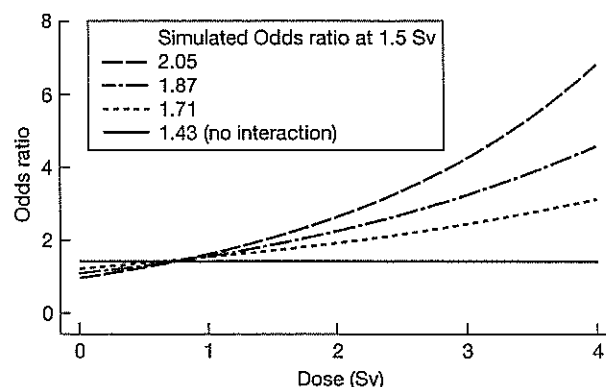


**Figure 2** The three levels of hypothetical oestradiol-radiation interaction used in the simulations. Plots show the odds ratio for oestradiol as a function of radiation dose. The overall odds ratio (1.43) for the case-control difference of 7% in log oestradiol value was set to occur at a dose of 0.75 Sv, near the median dose of the cases, corresponding to the result of the previous study

of interaction results in corresponding log OR of 0 and  $2.0\phi$  (OR = 1.00 and 2.05); it represents extreme effect modification in that it results in no oestradiol effect (OR = 1.0) among women not exposed to radiation.

We simulated 500 random case-control study outcomes for each of the 12 configurations defined by the number of controls per case selected (1, 2, 4, or 8) and the degree of interaction assumed (low, moderate, or high). All simulated data were generated using S-plus (MathSoft Inc., Seattle, Washington).

**Statistical analysis of simulated data**

We analysed the counter-matched design according to Langholz and Borgan,<sup>5</sup> using conditional logistic regression with sampling weights as offsets.<sup>15</sup> (An offset is added to the logistic

regression model by entering it as a covariate with coefficient fixed at 1.) Counter-matched sampling weights were calculated separately for each risk set ( $i, i = 1, \dots, I$ ), and exposure stratum ( $j, j = 1, \dots, J$ ) as:

$$\omega_{ij} = \log\{\text{number of cohort subjects in risk set } i \text{ and exposure stratum } j\}.$$

Weights are calculated in the same way for both cases and controls (Figure 1).

We studied effect modification via statistical interaction by fitting the model:

$$f(d, e) = \beta d + \theta e + \gamma de$$

where  $f(d, e)$  is the log odds of breast cancer,  $\beta$  is the log OR for a unit (1 Sv) difference in radiation dose ( $d$ ),  $\theta$  is the log OR for a unit difference in  $\log_{10}$ -oestradiol ( $e$ ), and  $\gamma$  is the interaction parameter. Interaction was tested by the  $\chi^2$  approximation to the likelihood ratio test of the null hypothesis  $\gamma = 0$ , which was rejected if the test statistic exceeded 3.84. Note that this is equivalent to failure of the likelihood-based CI to include the null value  $\gamma = 0$ . We calculated power as the proportion of 500 simulations in which the null hypothesis of no interaction was rejected. Because the power of a cohort based analysis—if oestradiol levels were known for all cohort members—would increase with increasing degree of interaction, we compared the power of each case-control design to that of the entire cohort. For each level of interaction we simulated 1000 cohort oestradiol values.

Counter-matched case-control samples were analysed using conditional logistic regression with weights as described above. Matched and randomly selected case-control samples were analysed using conditional logistic regression without weights. Cohort data were analysed using unconditional logistic regression. All analyses were conducted using Epicure (Hirosoft Inc., Seattle, Washington).

## Results

Figure 3 shows the distribution of randomly generated premenopausal oestradiol values for 80 cases and 160 controls from one set of 500 simulations assuming no interaction with radiation. There was substantial variation in simulated oestradiol levels within day and due to day of cycle. Oestradiol levels were 16% higher on average ( $\log_{10}$ -oestradiol values were 7% higher) in cases than in controls.

As shown in Table 1, compared with random selection of controls, the counter-matched and matched strategies increased power to detect interaction for each level of interaction when at least two controls per case were selected. All three methods demonstrated similar levels of power relative to the full cohort (slightly less than 40%) with only one control per case. Relative differences in power between the three strategies were similar regardless of the level of interaction. In Figure 4 we summarize the power of each design using curves fit to the average power (averaged over levels of interaction). Random control selection resulted in power that ranged from 50% of the cohort level with two controls per case to slightly more than 80% with eight controls per case. On the other hand, the exposure-based sampling strategies achieved levels of power ranging from almost 80% with two controls per case to 100% (maximum)

power with eight controls per case. For random sampling to achieve an acceptable level of power equivalent to that of the exposure-based control-selection designs required about twice as many controls, indicating that the exposure-based designs were about twice as efficient as random sampling for detecting interaction.

Repeated runs with counter matching and four controls per case with the moderate degree of interaction resulted in absolute power estimates of 0.466, 0.516, 0.518, 0.474, and 0.530 (average: 0.501, standard deviation 0.029). Because the variance of a binomial variable is a maximum when the proportion is 0.5, the other simulation results would be equally, or more, precise. The differences between exposure-related sampling designs and random sampling were much larger than this repeated simulation variability. However, differences between power for counter matching and matching were small and on the order of the simulation precision.

## Conclusions and Discussion

Case-control studies of interaction between multiple risk factors generally have low statistical power,<sup>16</sup> so designs that are suitably sized for studying main effects may be inadequate for studying effect modification.<sup>17</sup> The two exposure-related control-selection strategies studied here (matching and counter matching) resulted in similar gains in efficiency for testing interaction when two or more controls were selected per case. We conclude that, while more than 10 controls per case would be needed to achieve greater than 90% of the maximum, cohort level of power with random control selection, only 5–6 controls—about half as many as with random sampling—would be needed using either of the exposure-based control-selection designs. In practice, there could be missing specimens or refusal of informed consent, so using more than 5–6 controls per case might be considered based on the specific application. We do not recommend the use of only one control per case for studies of interaction.

The risk factors in our investigation were assumed to have positive interaction and one was a rare exposure already measured in the full cohort. This is the situation where matching performs best; in more general situations—i.e., when the two risk factors do not interact positively or when the matching factor is not rare—matching can lead to a loss of efficiency.<sup>4</sup> Counter matching generally improves statistical efficiency for studying interaction<sup>9</sup> and, unlike matching, further allows studying the exposure risk with adjustment for the other factor measured only in the case-control sample. Counter matching using sampling within risk-set strata is no more difficult to perform than matching on exposure, which can be complicated when additional risk-set matching factors are involved,<sup>11</sup> and both strategies require the use of conditional logistic regression. Counter matching additionally requires sampling weights, which are calculated from the numbers of cohort subjects in each risk-set exposure stratum in the cohort. Being able to examine the adjusted exposure risk would usually outweigh the extra effort involved in calculating the weights. We conclude that counter matching, and not matching, should generally be used to increase efficiency if a nested case-control study of joint effects is planned when one risk factor is known in the cohort.

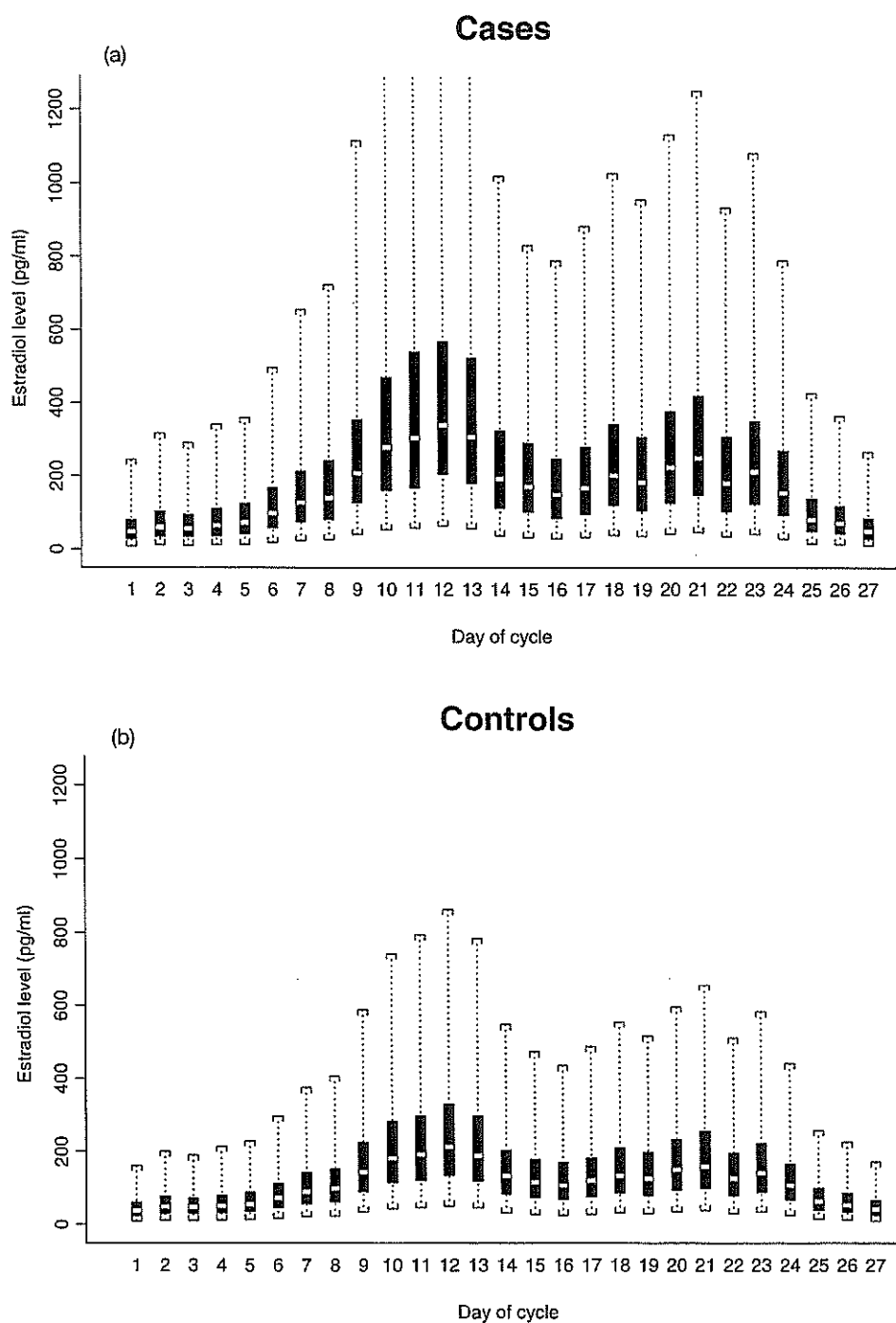


**Figure 3** Boxplots illustrating computer-generated oestradiol values by day of cycle among pre-menopausal breast cancer (a) cases and (b) selected controls. Data are from 500 simulations with 80 cases and 2 controls per case. Day of cycle is defined with 0 being 28 days prior to the start of the subsequent cycle (i.e. day 28 is the start of the next cycle). Case values are 16% higher on average than control values. The boxplots show the median (white dot), inter-quartile range (filled bar), and the most extreme observations (brackets)

When calculating the power of a study involving sampling from a cohort, two issues deserve consideration: power of the full cohort and power of the study design. There is little point in selecting a subset to investigate interaction if even the cohort is too small or the effect too weak to provide sufficient statistical

power. If the cohort has sufficient power, then the question becomes what type and size of design will provide the greatest possible efficiency within the limitations of financial cost, time, biological specimen availability, and other considerations. Breslow and Day point out that some sampling of cohort risk

**Table 1** Estimated power for detecting interaction relative to the full cohort for three control-selection strategies

Degree of interaction (cohort power)	Control-selection strategy	Control-to-case ratio			
		1	2	4	8
Low (0.293)	Random	0.40	0.54	0.75	0.92
	Matched	0.37	0.80	1.00	1.00
	Counter matched	0.36	0.78	1.00	1.00
Moderate (0.548)	Random	0.32	0.47	0.73	0.82
	Matched	0.34	0.77	1.00	1.00
	Counter matched	0.38	0.80	0.85	1.00
High (0.778)	Random	0.37	0.51	0.69	0.86
	Matched	0.35	0.70	0.96	1.00
	Counter matched	0.38	0.77	0.89	1.00

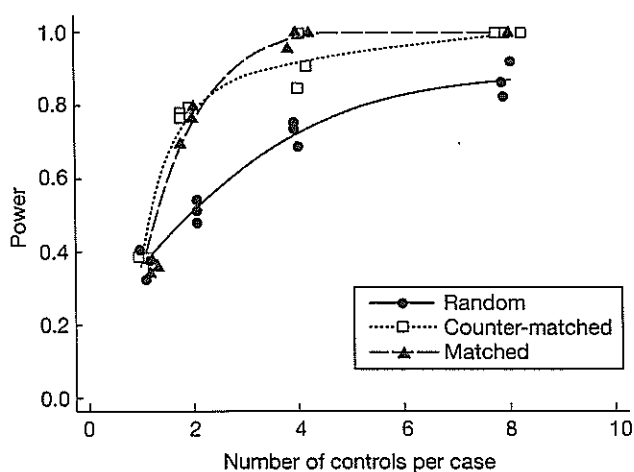


**Figure 4** Power of the control-sampling strategies for detecting interaction relative to the power of the full cohort. Points are values from Table 1, jittered slightly on the abscissa to reduce overlap. Lines are the results of fitting cubic power curves for purposes of smoothing the means (averaged over level of interaction)

sets can generally be performed with little loss of efficiency.<sup>18</sup> We have not considered the trade-off between cost and benefit here (see, for example, Reilly<sup>19</sup>), but in designing studies investigators must decide how much of the cohort power they are willing to sacrifice to achieve the necessary logistical savings. We have not investigated all possible designs, but for two approaches to nested case-control selection with fixed risk-set size, we have demonstrated that using counter matching can allow the researcher to achieve the same level of efficiency using about half as many controls as would be needed if controls were selected randomly.

The nested case-control design allows repeated selection of subjects in different risk sets; even cases can serve as controls in risk sets prior to their disease onset. Thus, there can be greater efficiency (in terms of number of subjects) depending on how many subjects are selected repeatedly by chance. In our application, the number of potential controls was large compared with the number of risk sets, so the probability of repeated selection was small. The total number of subjects needed for

a study will depend on this ratio as well as on the random draw of subjects. With matching, the number of potential controls at rare levels of exposure is limited and may lead to repeated selection. However, when counter matching is used, because dose strata are defined by quantiles, repeated selection is not likely to occur except for very large control:case ratios.

In studies with exposure known in the entire cohort, there is additional information on exposure risk in the non-selected subjects. Two-stage designs can improve efficiency.<sup>20-22</sup> Langholz and Goldstein<sup>23</sup> proposed a likelihood for analysing the case-control data only using a proportional odds model with multi-stage sampling. Land and others<sup>3</sup> proposed a method for incorporating the cohort risk estimate into the analysis of case-control subsets matched on exposure using more general risk models. There are also alternatives to the nested case-control design with counter matching. Borgan *et al.* addressed exposure-stratified selection in the case-cohort design.<sup>24</sup> Randomized recruitment as an alternative to counter matching can also result in efficiency gains.<sup>25</sup> Much remains to be done to synthesize the various designs and methods of analysis, but that is beyond the scope of the present work.

Because the present investigation was based on our interest in effect modification, we had to speculate as to what form it might take in order to simulate study power. Huang *et al.* reported that risk of breast cancer for medical irradiation to the chest in pre-/peri-menopausal women tended to be associated with oestrogen-receptor negative tumours,<sup>26</sup> suggesting that mechanisms other than those dependent on hormonal exposure may be involved. Radiation might cause additional genetic alterations that result in more rapid progression of breast cancer associated with oestrogen receptor negative phenotype. Oestrogen receptor negative breast cancer cells have been reported to be relatively resistant to IL-6 induced apoptosis,<sup>27</sup> so they may be more proliferative. If radiation induced alterations in signal transduction systems that were independent of the oestrogen receptor signalling system, then the joint effect of radiation and oestradiol could be multiplicative. If such alterations were dependent on the oestrogen receptor signalling system, then the joint effect could be greater than multiplicative. On the other hand, radiation exposure may lead to early onset of menopause,<sup>28</sup> which could indirectly reduce the risk of breast cancer by decreasing the duration of exposure to constitutional estrogens. Therefore,



in studying the joint effects of radiation and oestradiol, it is important to have sufficient power to detect or rule out interaction on the multiplicative scale to facilitate the planning of in-depth mechanistic studies.

Because these possibilities for interaction are mostly speculative, there was, in the present study, no basis to assume any particular type of effect modification between radiation and oestradiol. We therefore studied several arbitrary degrees of statistical interaction using a log-linear model. Effect modification can take other forms, including interaction on an additive scale. Such statistical interactions have been defined as effect-measure modification as distinguished from true effect modification, or biological interaction,<sup>29,30</sup> which implies that the joint effect of multiple risk factors exceeds the sum of their individual risks. In the analysis of data from a nested case-control study, one should consider alternatives to the standard log-linear logistic-regression model for the joint effect of multiple risk factors, such as additive or mixture models.<sup>31</sup>

In summary, we have demonstrated that matching and counter-matching on a known, continuous exposure variable provide equal gains in statistical power in a nested case-control study of risk-factor interaction with a control:case ratio of at least 2:1. However, matching on exposure prevents studying the effect of exposure after adjusting for one or more other risk

factors which might confound or modify the exposure risk, study aspects that counter matching addresses with greater efficiency than random sampling. We conclude that counter matching is superior to both matching on exposure and random control selection for nested case-control studies of effect modification when there is a known exposure.

## Acknowledgements

Special thanks go to Professor Bryan Langholz for advice and instruction regarding the method of counter matching. The study would not have been possible without the skilful technical support of Ms Sachiyo Funamoto. This publication was supported in part by research protocol 6-02 of the Radiation Effects Research Foundation (RERF), Hiroshima and Nagasaki, Japan. RERF is a private, non-profit foundation funded by the Japanese Ministry of Health, Labour and Welfare and the US Department of Energy, the latter through the National Academy of Sciences. The authors also acknowledge the support of Grants-in-Aid Nos. 14580356 and 14031227 from the Ministry of Education, Culture, Sports, Science, and Technology of Japan and grant number NCI-4893-8-001 from the US National Institutes of Health.

### KEY MESSAGES

- Selecting controls with consideration of a known, rare exposure can improve efficiency over random control selection in nested case-control studies of interaction.
- Counter matching produces the same gain in efficiency as matching for such studies but affords greater flexibility.
- Implementation of counter matching and estimation of power of a nested case-control study are illustrated using a case study of breast cancer and two risk factors, one of which is known in the cohort.

## References

- <sup>1</sup> Tokunaga M, Land CE, Tokuoka S, Nishimori I, Soda M, Akiba S. Incidence of female breast cancer among atomic bomb survivors, 1950-1985. *Radiat Res* 1994;138:209-23.
- <sup>2</sup> Key TJ, Verkasalo PK, Banks E. Epidemiology of breast cancer. *Lancet Oncol* 2001;2:133-40.
- <sup>3</sup> Land CE, Hayakawa N, Machado SG *et al*. A case-control interview study of breast cancer among Japanese A-bomb survivors. II. Interactions with radiation dose. *Cancer Causes Control* 1994;5:167-76.
- <sup>4</sup> Thomas DC, Greenland S. The efficiency of matching in case-control studies of risk-factor interactions. *J Chron Dis* 1985;38:569-74.
- <sup>5</sup> Langholz B, Borgan Ø. Counter-matching: A stratified nested case-control sampling method. *Biometrika* 1995;82:69-79.
- <sup>6</sup> Cologne JB. Counterintuitive matching (editorial). *Epidemiology* 1997;8:227-29.
- <sup>7</sup> Steenland K, Deddens JA. Increased precision using counter-matching in nested case-control studies. *Epidemiology* 1997;8:238-42.
- <sup>8</sup> Cologne J, Langholz B. Selecting controls for assessing interaction in nested case-control studies. *J Epidemiol* 2003;13:184-93.
- <sup>9</sup> Langholz B, Goldstein L. Risk set sampling in epidemiologic cohort studies. *Statist Sci* 1996;11:35-53.
- <sup>10</sup> Sharp GB, Neriishi K, Hakoda M *et al*. A nested case-control study of breast and endometrial cancer in the cohort of Japanese atomic bomb survivors. Research Protocol 6-02: Radiation Effects Research Foundation, Hiroshima, Japan; 2002.
- <sup>11</sup> Roesch WC (ed.). *US-Japan Joint Reassessment of Atomic Bomb Radiation Dosimetry in Hiroshima and Nagasaki*. Hiroshima, Japan: Radiation Effects Research Foundation, 1975.
- <sup>12</sup> Cologne JB, Shibata Y. Optimal case-control matching in practice. *Epidemiology* 1995;6:221-25.
- <sup>13</sup> Kabuto M, Akiba S, Stevens RG, Neriishi K, Land CE. A prospective study of estradiol and breast cancer in Japanese women. *Cancer Epidemiol Biomarkers Prev* 2000;9:575-79.
- <sup>14</sup> Verkasalo PK, Thomas HV, Appleby PN, Davey GK, Key TJ. Circulating levels of endogenous hormones and their relations to risk factors for breast cancer: a cross-sectional study in 1092 pre- and postmenopausal women (United Kingdom). *Cancer Causes Control* 2001;12:47-59.
- <sup>15</sup> McCullagh P, Nelder JA. *Generalized Linear Models*. 2nd Edn. London: Chapman and Hall, 1989.
- <sup>16</sup> Greenland S. Tests for interaction in epidemiologic studies: a review and a study of power. *Stat Med* 1983;2:243-51.
- <sup>17</sup> Smith PG, Day NE. The design of case-control studies: The influence of confounding and interaction effects. *Int J Epidemiol* 1984;13:356-65.

- <sup>18</sup> Breslow NE, Day NE. *Statistical Methods in Cancer Research. Volume II—The Design and Analysis of Cohort Studies*. Lyon: International Agency for Research on Cancer, 1987, pp. 200–02.
- <sup>19</sup> Reilly M. Optimal sampling strategies for two-stage studies. *Am J Epidemiol* 1996;**143**:92–100.
- <sup>20</sup> Breslow NE, Cain KC. Logistic regression for two stage case-control data. *Biometrika* 1988;**75**:11–20.
- <sup>21</sup> Zhao LP, Lipsitz S. Designs and analysis of two-stage studies. *Stat Med* 1992;**11**:769–82.
- <sup>22</sup> Breslow NE, Chatterjee N. Design and analysis of two-phase studies with binary outcome applied to Wilms tumour prognosis. *Appl Statist* 1999;**48**:457–68.
- <sup>23</sup> Langholz B, Goldstein L. Conditional logistic analysis of case-control studies with complex sampling. *Biostatistics* 2001;**2**:63–84.
- <sup>24</sup> Borgan Ø, Langholz B, Samuelsen SO, Goldstein L, Pogoda J. Exposure stratified case-cohort designs. *Lifetime Data Analysis* 2000;**6**:39–58.
- <sup>25</sup> Weinberg CR, Wacholder S. The design and analysis of case-control studies with biased sampling. *Biometrics* 1990;**46**:963–75.
- <sup>26</sup> Huang W-Y, Newman B, Millikan RC, Schnell MJ, Hulka BS, Moorman PG. Hormone-related factors and risk of breast cancer in relation to estrogen receptor and progesterone receptor status. *Am J Epidemiol* 2000;**151**:703–14.
- <sup>27</sup> Chiu JJ, Sgagias MK, Cowan KH. Interlukin 6 acts as a paracrine growth factor in human mammary carcinoma cell lines. *Clin Cancer Res* 1996;**2**:215–21.
- <sup>28</sup> Soda M, Cologne J. Radiation-accelerated age at menopause. *REF Update* 1993;**5**:5–6.
- <sup>29</sup> Rothman KJ. *Epidemiology: An Introduction*. Oxford: Oxford University Press, 2002; p. 170.
- <sup>30</sup> Greenland S, Rothman KJ. Concepts of interaction. In: Rothman KJ, Greenland S (eds). *Modern Epidemiology*. Philadelphia: Lippincott Williams & Wilkins, 1998; pp. 329–42.
- <sup>31</sup> Thomas DC. General relative-risk models for survival time and matched case-control analysis. *Biometrics* 1981;**37**:673–86.

Original Paper

# Allelic length of a CA dinucleotide repeat in the *egfr* gene correlates with the frequency of amplifications of this sequence — first results of an inter-ethnic breast cancer study

Horst Buerger,<sup>1\*</sup> Jens Packeisen,<sup>2</sup> Almuth Boecker,<sup>3</sup> Nicola Tidow,<sup>3</sup> Christian Kersting,<sup>1</sup> Krzysztof Bielawski,<sup>4</sup> Jorma Isola,<sup>5</sup> Yasushi Yatabe,<sup>6</sup> Kei Nakachi,<sup>7</sup> Werner Boecker<sup>1</sup> and Burkhard Brandt<sup>3</sup>

<sup>1</sup>Institute of Pathology, University of Muenster, Germany

<sup>2</sup>Institute of Pathology, Osnabrück, Germany

<sup>3</sup>Institute of Clinical Chemistry and Laboratory Medicine, University of Muenster, Germany

<sup>4</sup>Department of Biotechnology, University of Gdansk, Poland

<sup>5</sup>Institute of Medical Technology, University of Tampere, Finland

<sup>6</sup>Aichi Cancer Center Research Institute, Nagoya, Japan

<sup>7</sup>Department of Epidemiology, Saitama Cancer Center, Japan

\*Correspondence to:

Horst Buerger, MD, PhD,  
Institute of Pathology,  
Westfälische Wilhelmsuniversität  
Münster,  
Albert-Schweitzer-Strasse 33,  
48149 Münster, Germany.  
E-mail: buergerh@uni-muenster.de

## Abstract

Overexpression of the epidermal growth factor receptor (EGFR) is a common finding in invasive breast cancer and represents a potential target for new treatment options. However, little is known about the parameters that might indicate a potential clinical response for these anti-EGFR-based therapies. In order to gain further insights into the interplay between the length of a CA-SSR I repeat in intron 1 of *egfr*, copy numbers of this untranslated regulatory sequence, and protein expression, the present study investigated breast cancers from Germans and Japanese patients by microsatellite analysis, quantitative 5' nuclease assay by *egfr* enzyme-linked immunosorbent assay (ELISA), and comparative genomic hybridization (CGH). Japanese breast cancer patients displayed significantly longer alleles for the CA-SSR I repeat ( $p < 0.001$ ), associated with significantly lower EGFR expression (mean 65 versus 36 fmol/mg membrane protein). Allelic imbalance (restricted to CA-SSR I) was observed in 55% of the informative Japanese breast cancers compared with only 34% of the German breast cancer reference group. Using a quantitative 5' nuclease assay for *egfr*, a significantly higher percentage of Japanese breast cancer patients revealed amplifications of the CA-SSR I repeat ( $p < 0.01$ ). Japanese patients with these amplifications were characterized by a significantly higher EGFR content compared with the German breast cancer patients ( $p < 0.05$ ). These data show, on the one hand, that the correlation of EGFR overexpression and an inherited CA repeat polymorphism within intron 1 of *egfr* is a general finding in breast cancer, as has been shown previously. On the other hand, the data demonstrate clearly for the first time an interaction between the length of a polymorphism in intron 1 of *egfr* as an inherited genetic factor and the frequency of *egfr* amplification, as an acquired genetic factor, both factors contributing to EGFR overexpression in breast cancer. This new knowledge about mechanisms of regulation of EGFR expression might serve as an additional basis for evaluating anti-EGFR-based therapies.

Copyright © 2004 Pathological Society of Great Britain and Ireland. Published by John Wiley & Sons, Ltd.

Keywords: epidermal growth factor receptor; polymorphism; epidemiology

Received: 29 January 2003  
Revised: 26 November 2003  
Accepted: 8 December 2003

## Introduction

The epidermal growth factor receptor (EGFR) belongs to the *erbB* gene family and is overexpressed in a great variety of malignant tumours. In a number of studies investigating invasive breast cancer patients, overexpression of EGFR was found to correlate inversely with oestrogen receptor expression levels and positively with clinical outcome. Nevertheless, it was regarded as a prognostic factor of undetermined

significance [1–3]. The fact that its clinical value has not to date been estimated might be because the regulation of EGFR in cancer is not yet adequately understood [4].

In a previously published study, we investigated a polymorphic CA repeat in intron 1 of the epidermal growth factor receptor gene (*egfr* CA-SSR I), which determines the basal transcription activity of the *egfr* gene [1,5]. Moreover, we observed that allelic imbalances (AIs) restricted to the CA-SSR

I, as detectable by PCR-based microsatellite analysis, are a frequent event in breast cancer. They were even detectable in non-malignant breast tissue adjacent to invasive and *in situ* breast cancer [6]. Using gene dosage PCR, we determined that such AIs represented amplifications involving the regulatory sequence of intron 1. Additionally, inter-ethnic differences in the length of the CA dinucleotide repeat have been reported [7] and length differences between sporadic and familial breast cancer patients [8] have been described. Preliminary clinical observations also point towards a possible value of this polymorphism in the prediction of chemosensitivity [9,10].

Improved understanding of gene transcription and expression of *egfr* is required for clinical purposes, in view of the development, and clinical study, of new synthetic and antibody-based anti-EGFR therapies in recent years. These therapeutic approaches rely on optimal pre-therapeutic assessment of individual *egfr* status. A variety of technical approaches, including ELISA techniques and immunohistochemistry, as well as gene dosage measurements, have been published in the past. Only a limited number of somewhat contradictory studies have been published focusing on *egfr* amplifications; these have demonstrated that high-level amplifications of the whole gene are very rare events in breast cancer, in sharp contrast to its sister gene, *c-erbB2*.

In order to provide insights into the relationship between the length of the CA-SSR I in intron 1 of *egfr* and EGFR expression, we investigated breast cancer tissue from Japanese and German breast cancer patients. These features differ significantly between these ethnic subgroups, indicating that new diagnostic and predictive algorithms may need to be developed in the future.

## Materials and methods

Tumour and lymphocyte DNAs were extracted and used for further analysis after informed consent. The study protocol for the storage, analysis, and statistical evaluation of the samples was approved by the local ethical committees in Muenster, Nagoya, and Saitama.

### Determination of the number of CA repeats in intron I

The germ line allele status of the polymorphic CA repeat within intron 1 of *egfr*, being a fragment of 114–138 bp (by PCR) containing the CA dinucleotide repeat, was determined as described elsewhere in 180 German and 126 Japanese breast cancer patients [1]. Separation was achieved using a four-colour laser-induced fluorescence capillary electrophoresis system (Prism 3700; ABI, Weiterstadt, Germany) employing GeneScan Standard TAMRA-500 for fragment length evaluation. Evaluation was performed using GeneScan™ 2.1 evaluation software (ABI, Weiterstadt, Germany).

### Determination of loss of heterozygosity (LOH) in intron I

Tumour DNA and DNA from blood lymphocytes were isolated with the QIAamp Tissue Kit (Quiagen, Hilden, Germany) from 43 Japanese breast cancer patients. A 114–132 bp PCR fragment containing the polymorphic region was amplified with 50 pmol of established primers [11] and evaluated for allele scoring and assessment of LOH as described elsewhere [1,12].

### Determination of EGFR expression (ELISA)

EGFR content in breast cancer samples was analysed in 30 Japanese and 30 German tumour samples. The samples were pair-matched by menopausal status, histological grade, and oestrogen receptor status. All samples were analysed in the same run. Protein isolation and the ELISA for the determination of EGFR expression were carried out as described elsewhere [1].

### Quantitative real-time PCR (5' nuclease assay)

Primers specific for sequences flanking the first CA repeat in the first intron of the *egfr* gene (CAIfor: 5'-TGAAGAATTTGAGCCAACCAAA-3' and CAIrev: 5'-CACTTGAACCAGGGACAGCA-3') were designed using Primer Express software (Applied), and a universal probe consisting of 15 CA repeats as well as a 5' fluorescent label (CA-Fam) was also established. Primers and probes were also designed for two different single-copy genes, manganese superoxide dismutase (SOD2, chromosome 6q25, GenBank accession No 65 965) and beta-globin (HBB, chromosome 11p, GenBank accession No V00499). The 5' nuclease assay including the appropriate controls was performed as previously described [6]. DNA concentrations were normalized with respect to both SOD2 and HBB, two different single-copy genes [13].

### Statistical tests

Statistical analysis was carried out using the Wilcoxon rank test, Student's *t*-test and the chi-square-test. *p* values less than 0.05 were considered significant.

## Results

### Comparison of the frequency of allelic imbalance (AI) at CA-SSR I as determined by PCR-based microsatellite analysis

Sixty-two per cent of the Japanese breast tumours were heterozygous (informative) for the microsatellite analysed. As such, 55% of these tumours revealed AI at CA-SSR I. However, in the previously reported German comparator group, 88% of tumours were heterozygous but AI at CA-SSR I was present in only 34% (*p* < 0.01) [1,6].

AI at CA-SSR I represents amplification as determined by quantitative real-time PCR

AI assessed by PCR-based microsatellite analysis describes only the relative gene dosages of the two CA-SSR I alleles. To determine whether the AI represents amplification or deletion, we performed a quantitative 5' nuclease assay. *egfr*-specific primers that flank the CA-SSR I in the first intron as well as a FAM-labelled (CA)<sub>15</sub> probe were used in this assay. PCR amplification was performed using serial dilutions of leukocyte and tumour DNA normalized with respect to two different housekeeping genes as described in the Materials and methods section.

The sensitivity of the method allows the detection of amplification if the LOH score is less than 0.56 or more than 1.3. As a control, DNA isolated from the MDA-MB-468 cell line was tested and displayed 30- to 60-fold amplification of *egfr* CA-SSR I. Because of the limited sensitivity of the 5' nuclease assay, amplification could be confirmed in only one-third of cases presenting with AI. However, no tumour with a decreased gene dosage was found by this method. Moreover, the 5' nuclease assay assessed a 16- to 32-fold increase in the gene dosage of *egfr* in the two tumours with high-level gains of *egfr*, as detected by CGH (Figures 1 and 2).

#### Distribution of the length of the polymorphic CA dinucleotide stretch at CA-SSR I in German and Japanese breast cancer patients

Comparison of the length of the CA dinucleotide repeat at CA-SSR I yielded a highly significant difference in the germ line allele status between the German and the Japanese patient groups. Tumours from German women harboured, on average, shorter stretches containing 16–18 CA dinucleotides (71.6%) than Japanese women. The Japanese tumours were very homogeneous, with predominantly longer alleles containing 19 or more CA dinucleotides, which covered 67% of all alleles (Figure 3;  $p < 0.001$ , Wilcoxon test).

#### Regulation of EGFR expression is associated with allele length and CA-SSR I amplification in German and Japanese tumours

In order to investigate the interplay between *egfr* CA-SSR I length, amplification of the *egfr* CA-SSR, and EGFR expression, we determined the intratumoural EGFR concentration using an enzymatic immunoassay. Significantly lower EGFR expression levels were found in the Japanese tumours than in the German breast cancers (Figure 3; median: 17 versus 59; mean  $\pm$  SEM:  $24 \pm 12$  versus  $65 \pm 35$  fmol/mg,  $p < 0.001$ , Wilcoxon test).

In contrast, the Japanese breast tumours that harboured amplifications of the *egfr* CA-SSR I as assessed by the 5' nuclease assay expressed significantly higher EGF receptor densities compared with

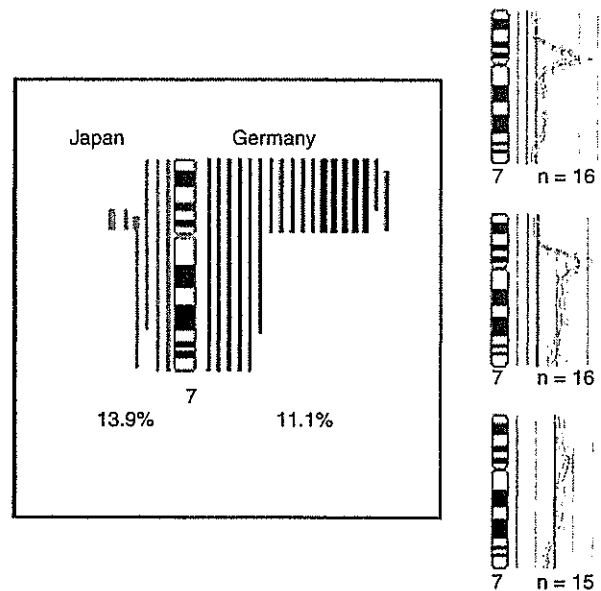


**Figure 1.** Left: all gains of chromosomal material including 7p in German and Japanese breast tumours are indicated on both sides of the ideogram of chromosome 7 in a cumulative manner. High-level amplifications are indicated using thick bars. The overall frequency of 7p-gains in both subgroups is given below the ideogram. Right: the respective CGH ratio profiles of chromosome 7 for all Japanese patients with high-level amplification of *egfr* are shown. The black central line indicates the fluorescence ratio of balanced DNA sequence copy number state (1.0) between the tumour and reference DNA. The lines to the left represent the 0.75 and 0.5 thresholds for losses, and the lines to the right the 1.25, 1.5, 1.75, etc. thresholds for gains. 95% confidence limits are shown. Chromosome numbers are also indicated. Whereas two Japanese breast tumours demonstrated clear high-level amplifications similar to MDA-MB-468, one case showed a circumscribed low-level gain of genetic material in 7p12–13

the German cases (mean  $\pm$  SEM:  $113.5 \pm 31.2$  versus  $65 \pm 35$  fmol/mg;  $p < 0.05$ , *t*-test; median: 96.1 versus 59 fmol/mg;  $p < 0.05$ , Wilcoxon test).

#### Discussion

Members of the *erbB* gene family are attractive targets for new therapeutic strategies in various malignant neoplasms, since their overexpression, especially in breast cancer, is a common finding [14]. The clinical application of such new specific treatment modalities is unfortunately hampered by restricted knowledge regarding reliable diagnostics for identifying those patients who might benefit from such approaches [15].

For *c-erbB2*, the evaluation of immunohistochemical expression and gene dosage measurements by fluorescence *in situ* hybridization (FISH) currently represents the state-of-the-art [16]. For EGFR, the situation is much more complicated. Patients with EGFR overexpression seem to be independent of those with *c-erbB2* expression [17,18]. Investigation of breast